Combination and summary of ATLAS dark matter searches interpreted in 2HDM+a

The 9th CLHCP Workshop

Khanh N. Vu
on behalf of the ATLAS Collaboration

November 19th, 2023

Outline

1. Introduction on 2HDM+a

2. Experimental signatures

3. Statistical combination of results

4. Summary of constraints on 2HDM+a

EUROPEAN ORGANISATION FOR NUCLEAR RESEARCH (CERN)

Submitted to: Science Bulletin

CERN-EP-2023-088
2nd June 2023

Combination and summary of ATLAS dark matter searches interpreted in a 2HDM with a pseudo-scalar mediator using 139 fb^{-1} of $\sqrt{s} = 13$ TeV pp collision data

The ATLAS Collaboration

Results from a wide range of searches targeting different experimental signatures with and without missing transverse momentum ($E_{\text{T}}^{\text{miss}}$) are used to constrain a Two-Higgs-Doublet Model (2HDM) with an additional pseudo-scalar mediating the interaction between ordinary and dark matter (2HDM+a). The analyses use up to 139 fb^{-1} of proton–proton collision data at a centre-of-mass energy $\sqrt{s} = 13$ TeV recorded with the ATLAS detector at the Large Hadron Collider during 2015–2018. The results from three of the most sensitive searches are combined statistically. These searches target signatures with large $E_{\text{T}}^{\text{miss}}$ and a leptonically decaying Z boson; large $E_{\text{T}}^{\text{miss}}$ and a Higgs boson decaying to bottom quarks; and production of charged Higgs bosons in final states with top and bottom quarks, respectively. Constraints are derived for several common and new benchmark scenarios in the 2HDM+a.

arXiv:2306.00641

accepted by Science Bulletin (1st time by ATLAS on this Chinese SCI journal)

© 2023 CERN for the benefit of the ATLAS Collaboration.
Reproduction of this article or parts of it is allowed as specified in the CC-BY-4.0 license.

Introduction

- Dark Matter: supported by many of astrophysical measurements; SM is insufficient to explain ⟶ strong consideration in many BSM extensions.

- Complementary probes of DM in several areas

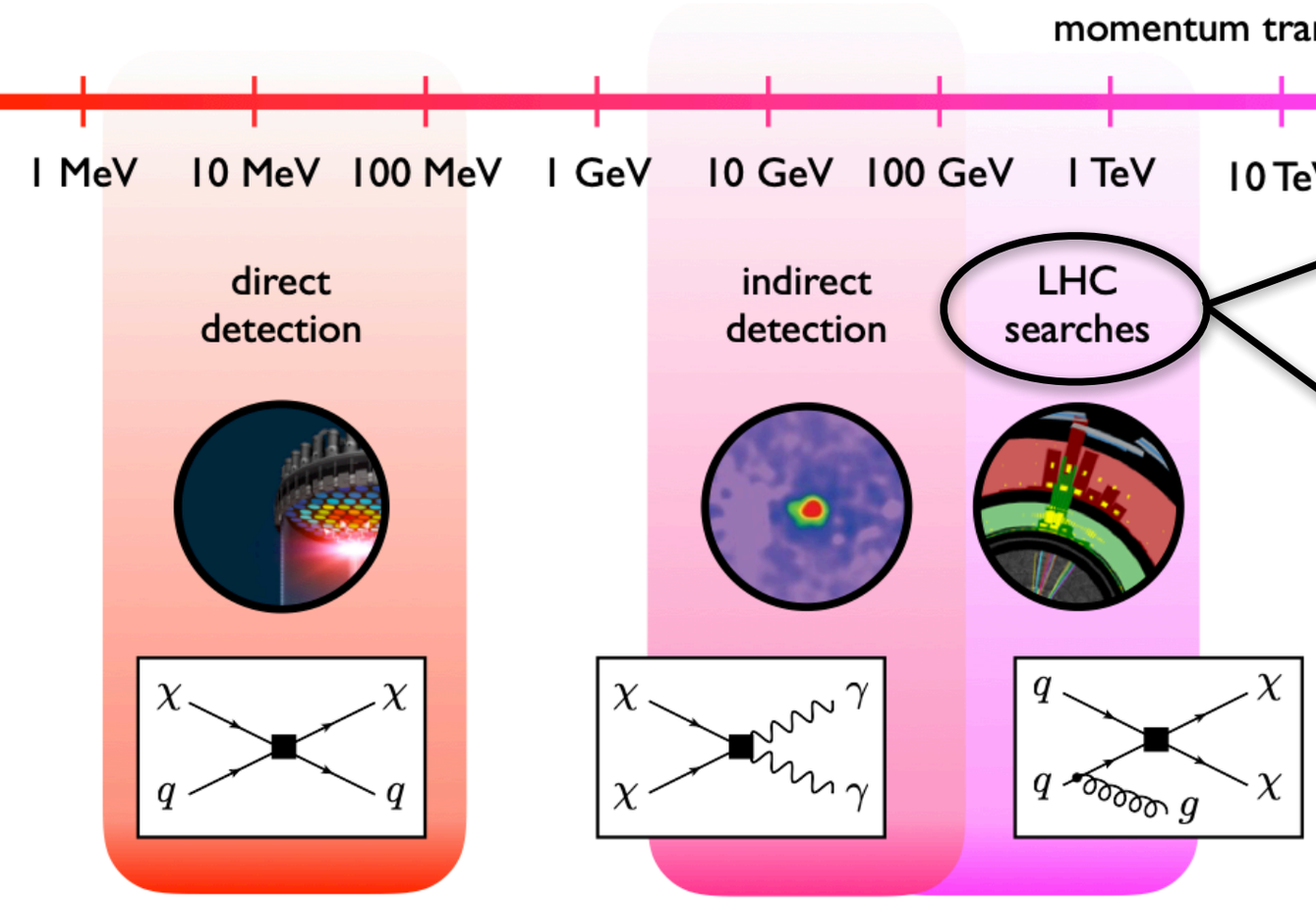

- ATLAS sensitive to wide variety of DM, especially WIMPs.
  - relic density → WIMP mass ∼ EWK scale.

- provide access to nature of DM↔SM interaction (*mediator*), via
  - $E_{\mathrm{T}}^{\mathrm{miss}} + X$ (mono-X, mediator → invisible)
  - Resonance / decay product reconstruction (mediator → visible).

$E_{\mathrm{T}}^{\mathrm{miss}}$: missing transverse momentum

2HDM+a

- In this talk, ATLAS DM searches interpreted in **Two-Higgs-Doublet Model plus a pseudo-scalar mediator (2HDM+a)**:
  - Minimal, UV-complete extension.
  - EWK Symmetry Breaking:
    - 5 Higgs: $h, H, H^{\pm}, A$
    - 1 light pseudo-scalar: a

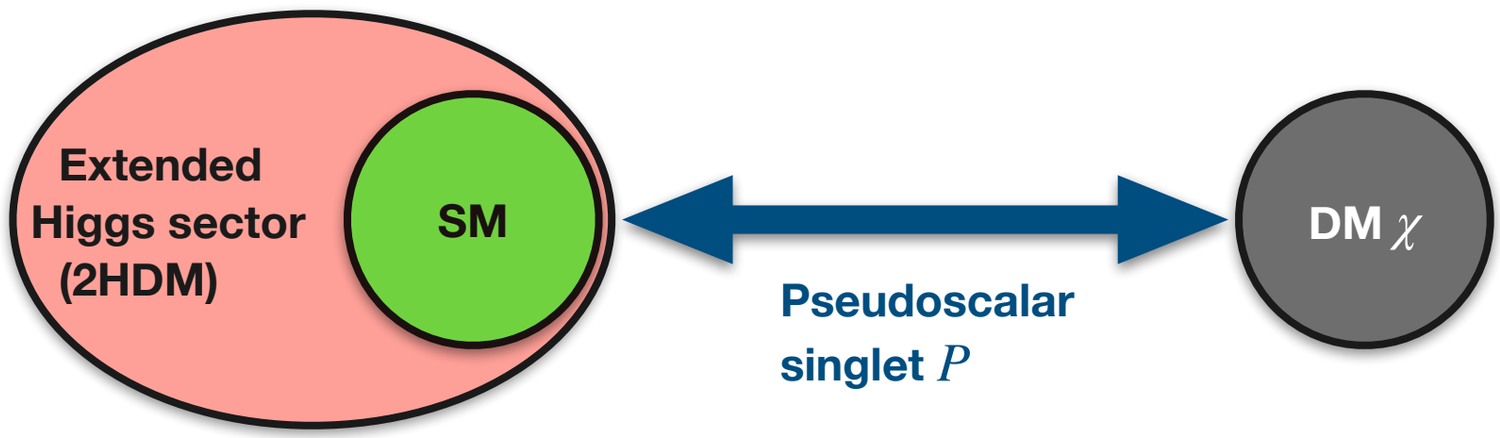

2HDM+a fully defined by 14 parameters

$$v,\ M_h,\ M_A,\ M_H,\ M_{H^\pm},\ M_a,\ m_\chi$$
$$\cos(\beta-\alpha),\ \tan\beta,\ \sin\theta,$$
$$y_\chi,\ \lambda_3,\ \lambda_{P1},\ \lambda_{P_2}$$

EWK, flavour constraints and to simplify parameter space

5 unconstrained parameters

$m_A = m_H = m_{H^\pm}$	masses of heavy Higgs
m_a	mass of pseudo-scalar mediator
m_χ	DM mass
$\sin\theta$	mixing angle between CP-odd states a and A
$\tan\beta$	ratio of 2 Higgs doublet VEVs

LHC Dark Matter Working Group
Phys. Dark Univ. 27 (2020) 100351
Bauer, Haisch, Kahlhoefer
JHEP05(2017) 138

*h: SM-like CP-even Higgs with mass of 125 GeV

Experimental signatures

- 2HDM+a has rich phenomenology predicting wide range of signatures with both visible and invisible decays
  - resonantly production of $E_{\mathrm{T}}^{\mathrm{miss}} + Z/h$
  - additional (pseudo-)scalar bosons, e.g $tbH^{\pm}(tb)$
  - new signatures, e.g $E_{\mathrm{T}}^{\mathrm{miss}} + tW$

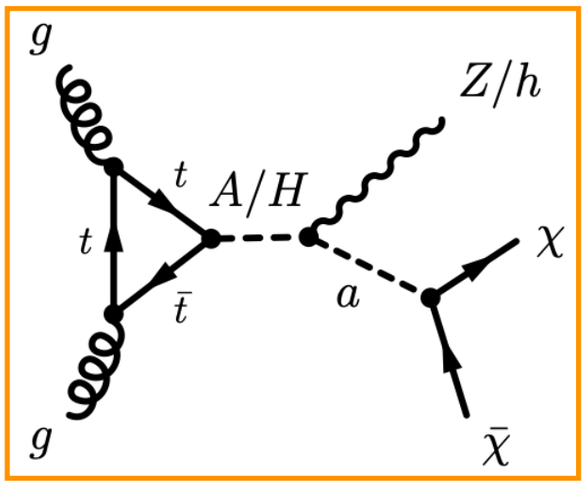

$E_{\mathrm{T}}^{\mathrm{miss}} + Z/h$

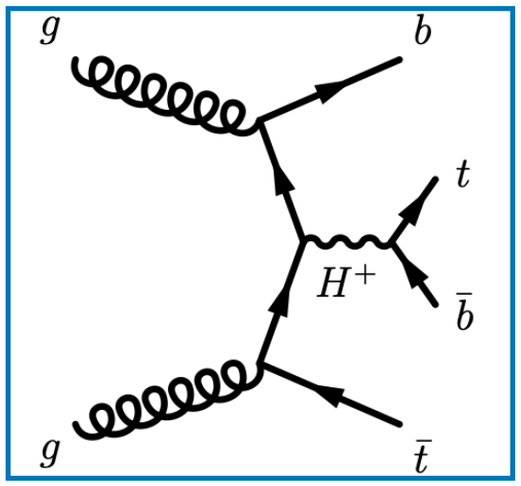

$tbH^{\pm}(tb)$

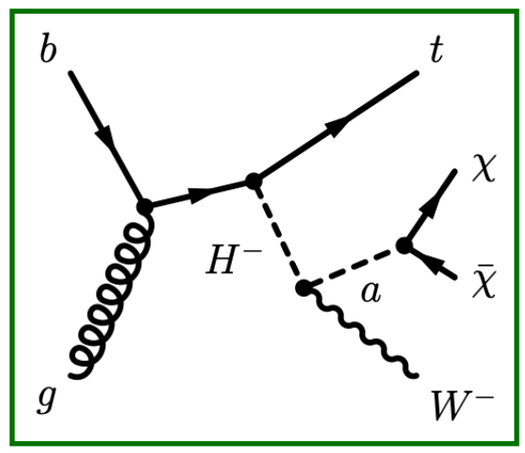

$E_{\mathrm{T}}^{\mathrm{miss}} + tW$

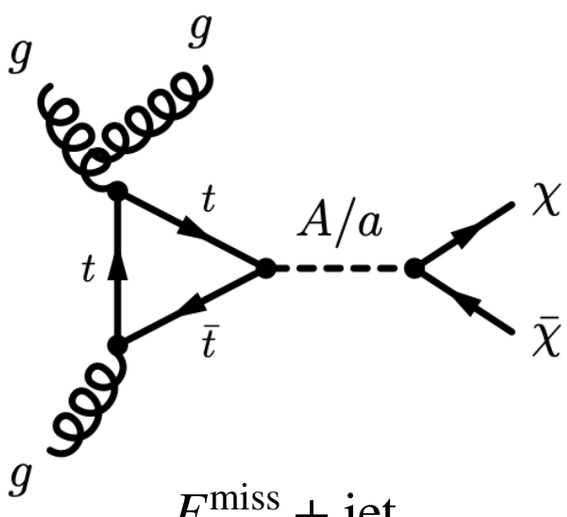

$E_{\mathrm{T}}^{\mathrm{miss}} + \mathrm{jet}$

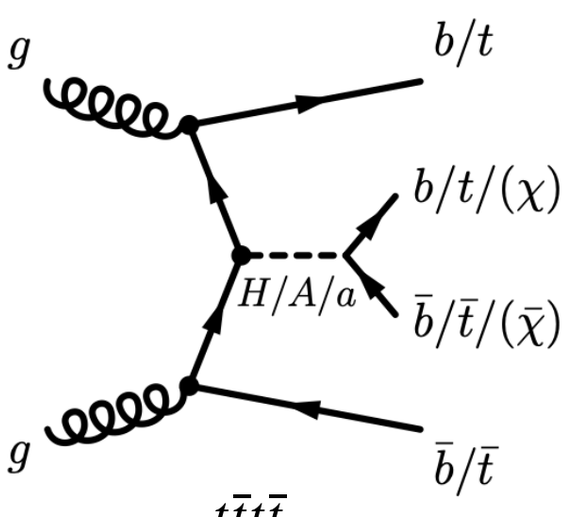

$t\bar{t}t\bar{t}$

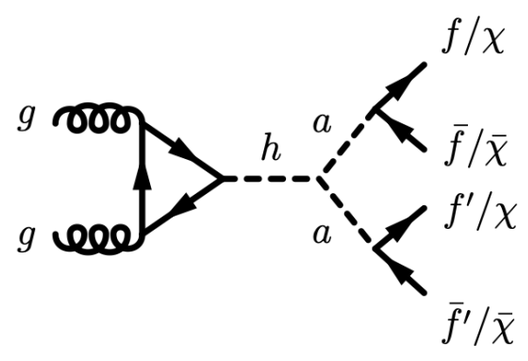

$h \to aa \to 4f\,/\,h \to \mathrm{invisible}$

$E_{\mathrm{T}}^{\mathrm{miss}} + Z(ll)$ signature

Phys. Lett. B 829 (2022) 137066

- **Signal region**:
  - Z boson recoiling against large $E_{\mathrm{T}}^{\mathrm{miss}}$ > 90 GeV
  - Presence of a pair of high-p_{T}, same flavour, oppositely charged leptons with angular separation < 1.8

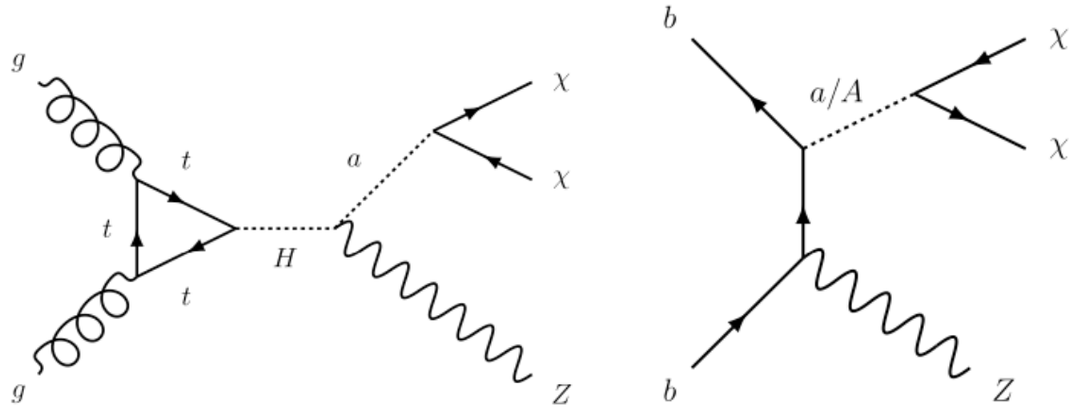

gg-initiated bb-initiated

- Dominant bkgs ZZ, WZ and non-resonant bkgs estimated using **4l, 3l, and eμ Control Regions.**

- Fit to data is performed on $m_{\mathrm{T}}^{\mathrm{lep}}$ (in SR and $e\mu$ CR) + $E_{\mathrm{T}}^{\mathrm{miss}}$ (in 4l and 3l CRs).

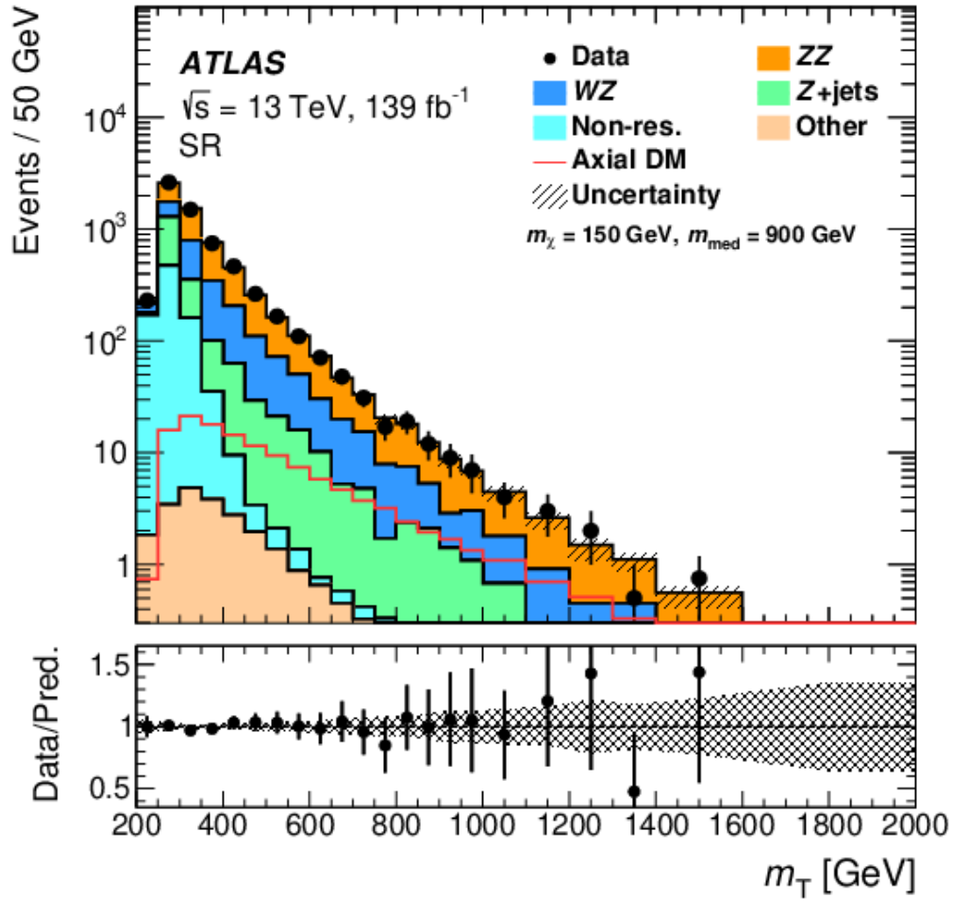

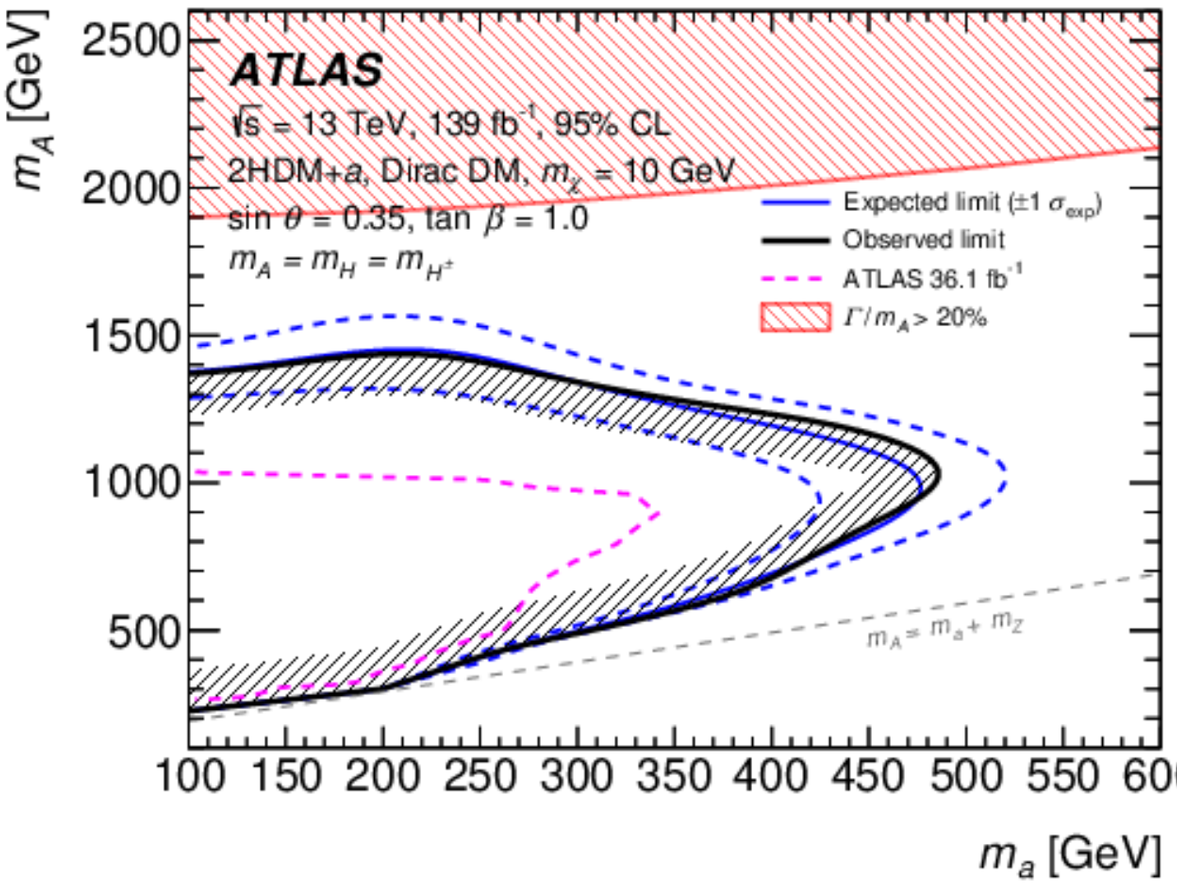

$$m_{\mathrm{T}}^{\mathrm{lep}} = \sqrt{\left[\sqrt{m_{\mathrm{Z}}^2 + (p_{\mathrm{T}}^{\ell\ell})^2} + \sqrt{m_{\mathrm{Z}}^2 + (E_{\mathrm{T}}^{\mathrm{miss}})^2}\right]^2 - \left[\vec{p}_{\mathrm{T}}^{\,\ell\ell} + \vec{p}_{\mathrm{T}}^{\,\mathrm{miss}}\right]^2}$$

$E_{\mathrm{T}}^{\mathrm{miss}} + h(bb)$ signature

JHEP 11 (2021) 209

- **Signal Regions:**
  - Higgs boson recoiling against large $E_{\mathrm{T}}^{\mathrm{miss}}$ > 150 GeV
  - categorized into == 2 b-jets or > 2 b-jets targeting both gg-induced and bb-induced production; each then split in ortho. $E_{\mathrm{T}}^{\mathrm{miss}}$ bins.
  - **Higgs decay reconstructed as single large-R jet for $E_{\mathrm{T}}^{\mathrm{miss}}$ > 500 GeV**

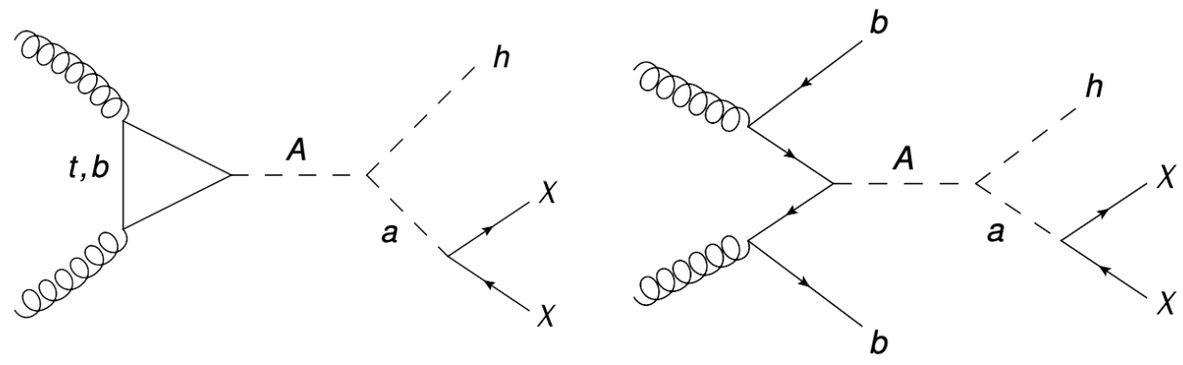

gg-induced bb-induced

- Dominant bkgs $t\bar{t}$ and $W/Z + \mathrm{jet}_{\mathrm{hf}}$ estimated using **1l and 2l Control Regions.**
- Fit to data on m_{bb} (in SRs) + event yields (in CRs).

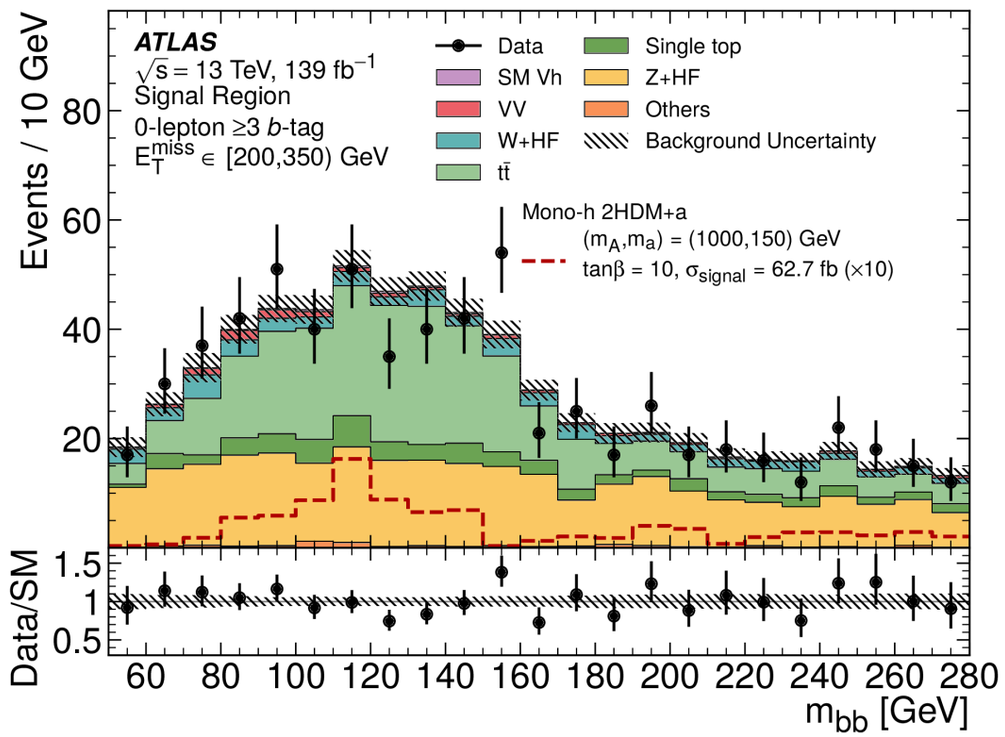

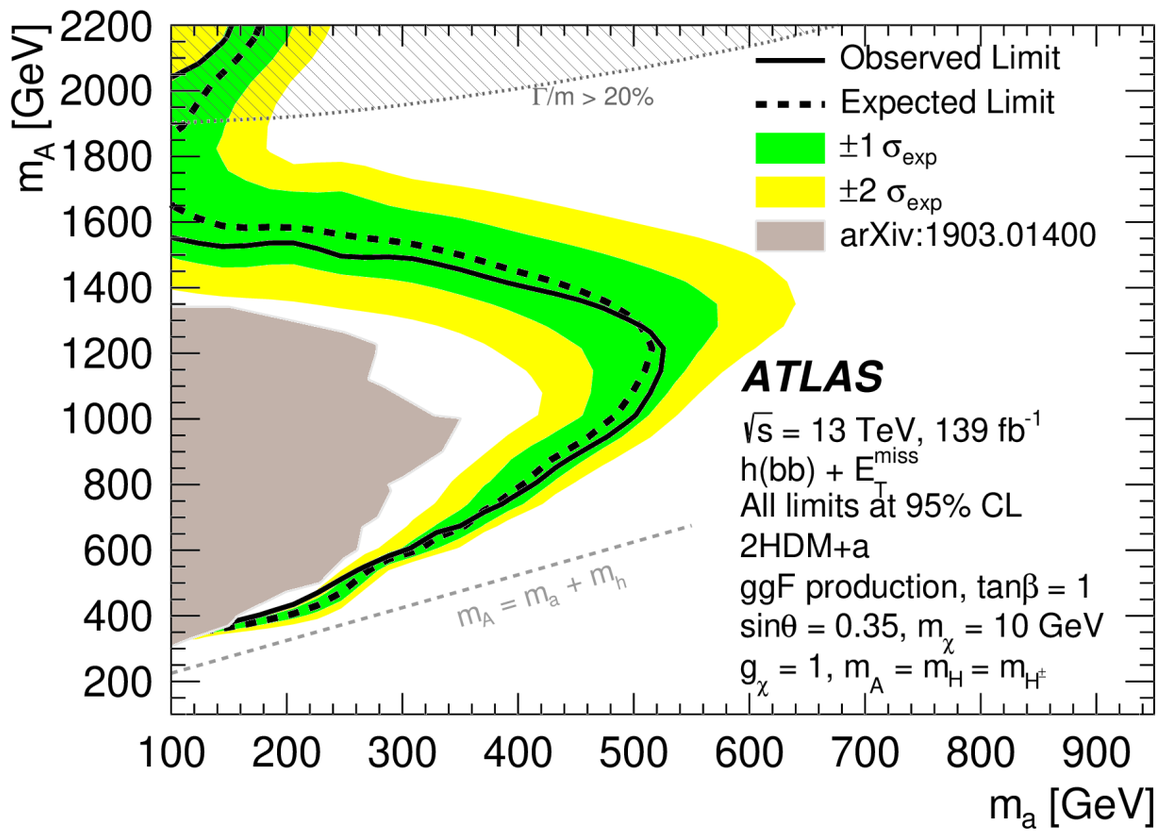

$tbH^{\pm}(tb)$ signature

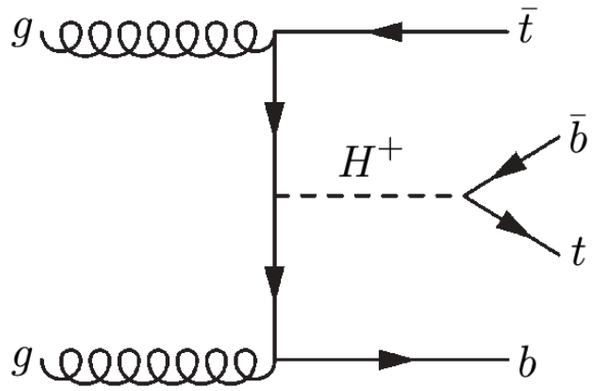

JHEP 06 (2021) 145

- original analysis for 2HDM type-II, searching heavy charged Higgs, mass in [0.2, 2] TeV.
  - re-interpreted for 2HDM+a by rescaling 2HDM type-II exclusion limits.

- **Signal Regions**:
  - **1l + $\geq$ 5j + $\geq$ 3b** to target semi-leptonic decay of one of top quarks
  - **4 separate SRs** according to jet and b-jet multiplicity.
  - **A Neural Network** used to enhance discrimination between signals and bkgs.

- **Dominant bkg $t\bar{t}$ + jets estimated using data-driven corrections obtained in >=5j2b regions.**

- Fit to data performed on NN distributions across regions.

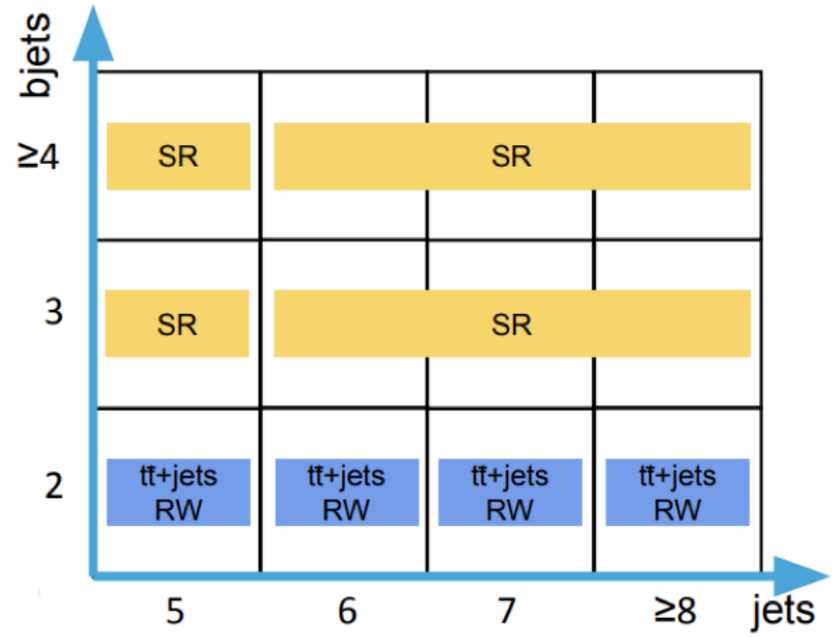

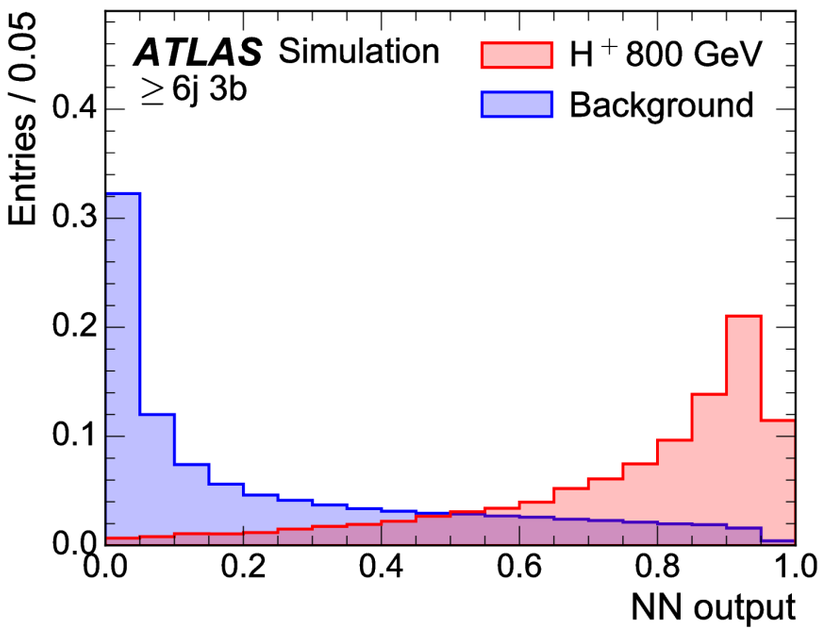

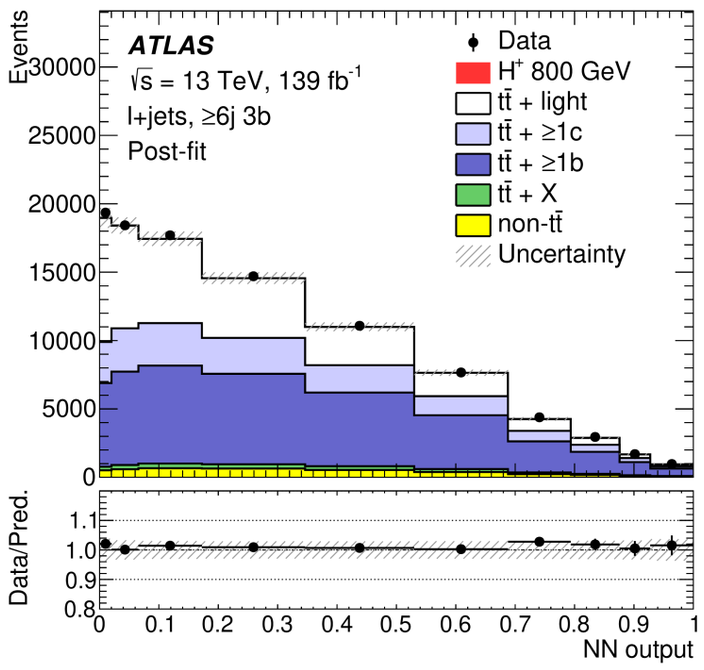

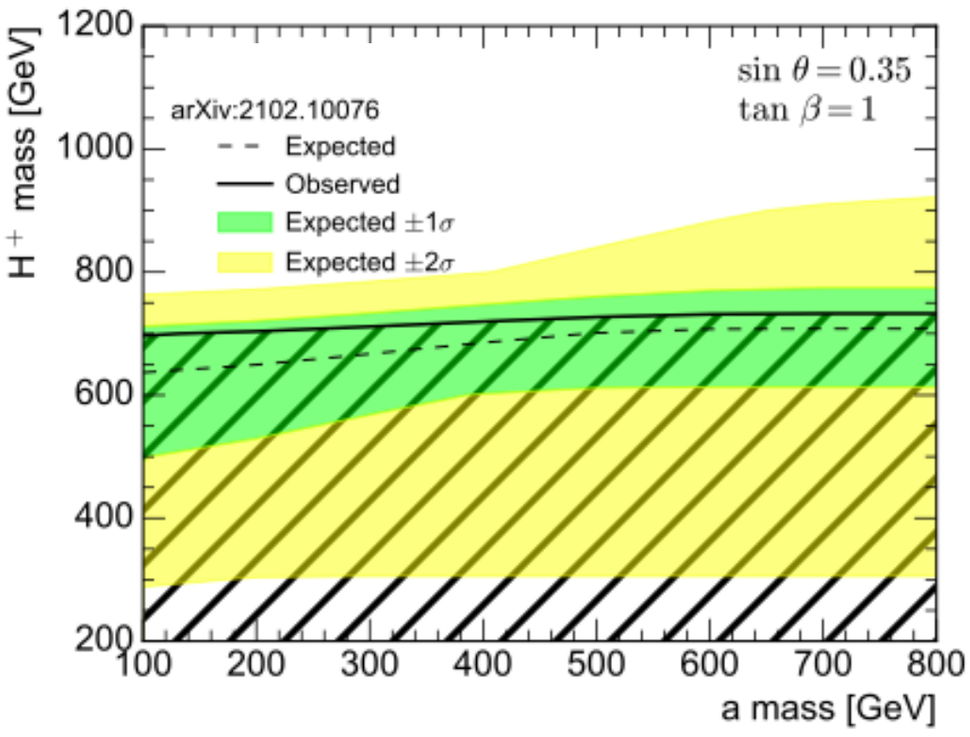

Statistical combination

- $E_{\mathrm{T}}^{\mathrm{miss}} + h(bb)$, $E_{\mathrm{T}}^{\mathrm{miss}} + Z(ll)$ and $tbH^{\pm}(tb)$: Most constraining signatures of 2HDM+a.
  - $tbH^{\pm}(tb)$ gives significant complementarity to sensitivities of $E_{\mathrm{T}}^{\mathrm{miss}} + X$
  - stat. combination of 3 channels to maximize 2HDM+a constraints in parameter space.
- Combined exclusion limits obtained from **profile likelihood ratio** corresponding to **3-channel-combined likelihood**.
- Decorrelate over-constrained/pulled uncertainties to avoid any phase-space-specific biases across channels.

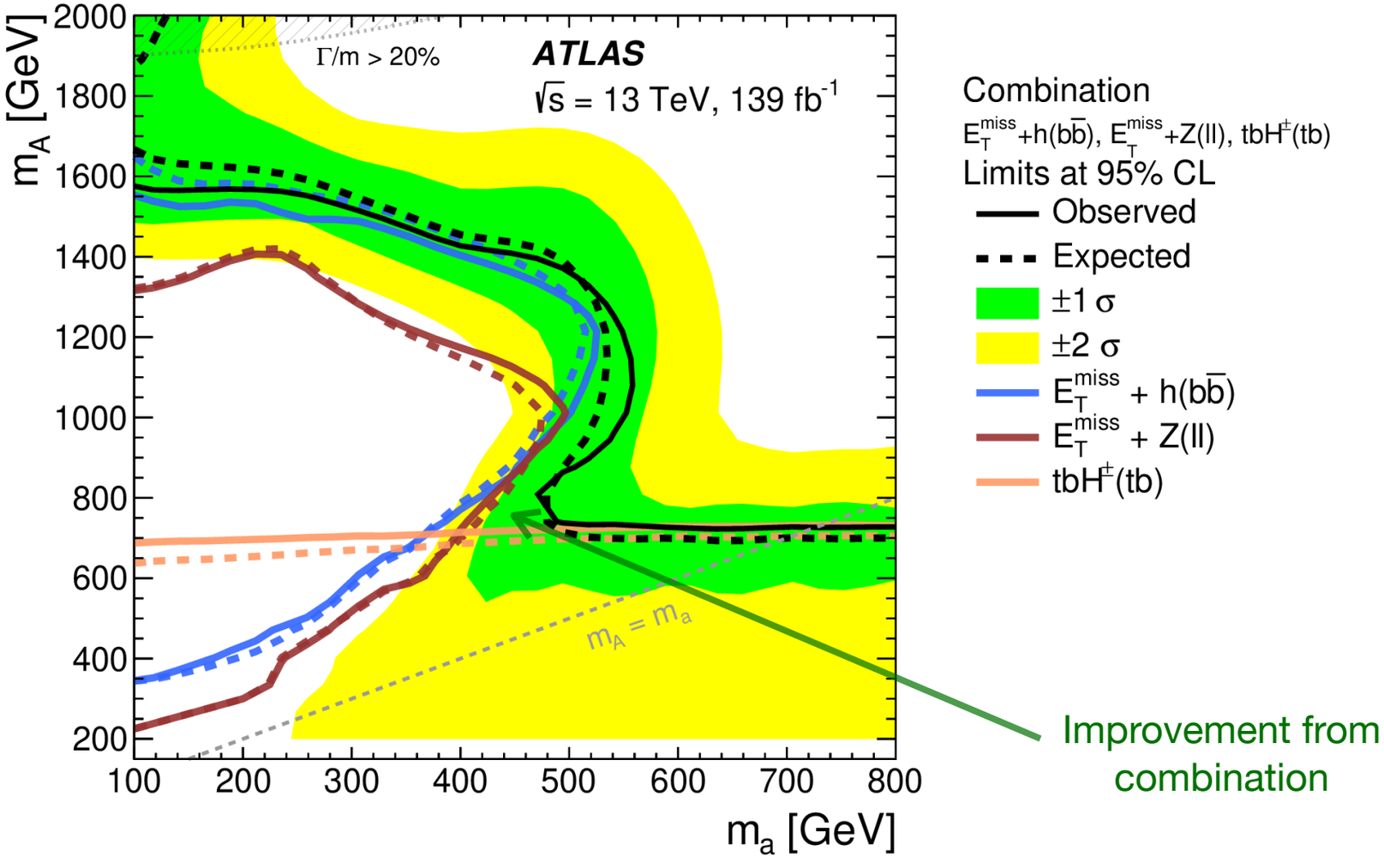

Summary of constraints on 2HDM+a

- constraints on 2HDM+a interpreted in **6 benchmark scenarios**.
  - highlight diverse phenomenology of 2HDM+a.
  - study the interplay and complementarities between different signatures.

Scenario		Fixed parameter values				Varied parameters
		$\sin\theta$	m_A [GeV]	m_a [GeV]	$\tan\beta$	
1	a	0.35	–	–	1.0	(m_a, m_A)
	b	0.70	–	–	1.0	
2	a	0.35	–	250	–	$(m_A, \tan\beta)$
	b	0.70	–	250	–	
3	a	0.35	600	–	–	$(m_a, \tan\beta)$
	b	0.70	600	–	–	
4	a	–	600	200	1.0	$\sin\theta$
	b	–	1000	350	1.0	
5		0.35	1000	400	1.0	m_χ
6		0.35	1200	–	1.0	(m_a, m_χ)

shows interplay due to mass hierarchies

motivated by similar scans done for general 2HDMs

illustration a-A mixing parameter effect

connection with cosmological constraints and direct/indirect searches

showed for the 1st time

m_χ set to 10 GeV in all scenarios, except 5 and 6

Summary of constraints on 2HDM+a

Variety of searches interpreted in the context of different 2HDM+a benchmark scenarios

Analysis/Scenario	1a	1b	2a	2b	3a	3b	4a	4b	5	6
$E_{\mathrm{T}}^{\mathrm{miss}} + Z(\ell\ell)$ [74]	x	x	x	x	x	x	x	x	x	
$E_{\mathrm{T}}^{\mathrm{miss}} + h(b\bar{b})$ [75]	x	x	x	x	x	x	x	x	x	x
$E_{\mathrm{T}}^{\mathrm{miss}} + h(\gamma\gamma)$ [84]	x	x			x	x	x	x		
$E_{\mathrm{T}}^{\mathrm{miss}} + h(\tau\tau)$ [78]	x			x						
$E_{\mathrm{T}}^{\mathrm{miss}} + tW$ [77]	x	x	x	x	x	x	x	x		
$E_{\mathrm{T}}^{\mathrm{miss}} + j$ [45]	x	x			x	x	x	x		
$h \to$ invisible [86]	x	x			x					x
$E_{\mathrm{T}}^{\mathrm{miss}} + Z(q\bar{q})$ [127]	x						x	x		
$E_{\mathrm{T}}^{\mathrm{miss}} + b\bar{b}$ [128]							x	x		
$E_{\mathrm{T}}^{\mathrm{miss}} + t\bar{t}$ [128,129]							x	x		
$t\bar{t}t\bar{t}$ [85]	x	x	x	x	x	x	x	x	x	
$tbH^{\pm}(tb)$ [76]	x	x	x	x	x	x	x	x	x	
$h \to aa \to f\bar{f}f'\bar{f}'$ [79,80,81,82,83]										x

Scenario 1a: $\sin\theta = 0.35$ m_A-m_a plane

- $h \rightarrow$ invisible constrains very low m_a.

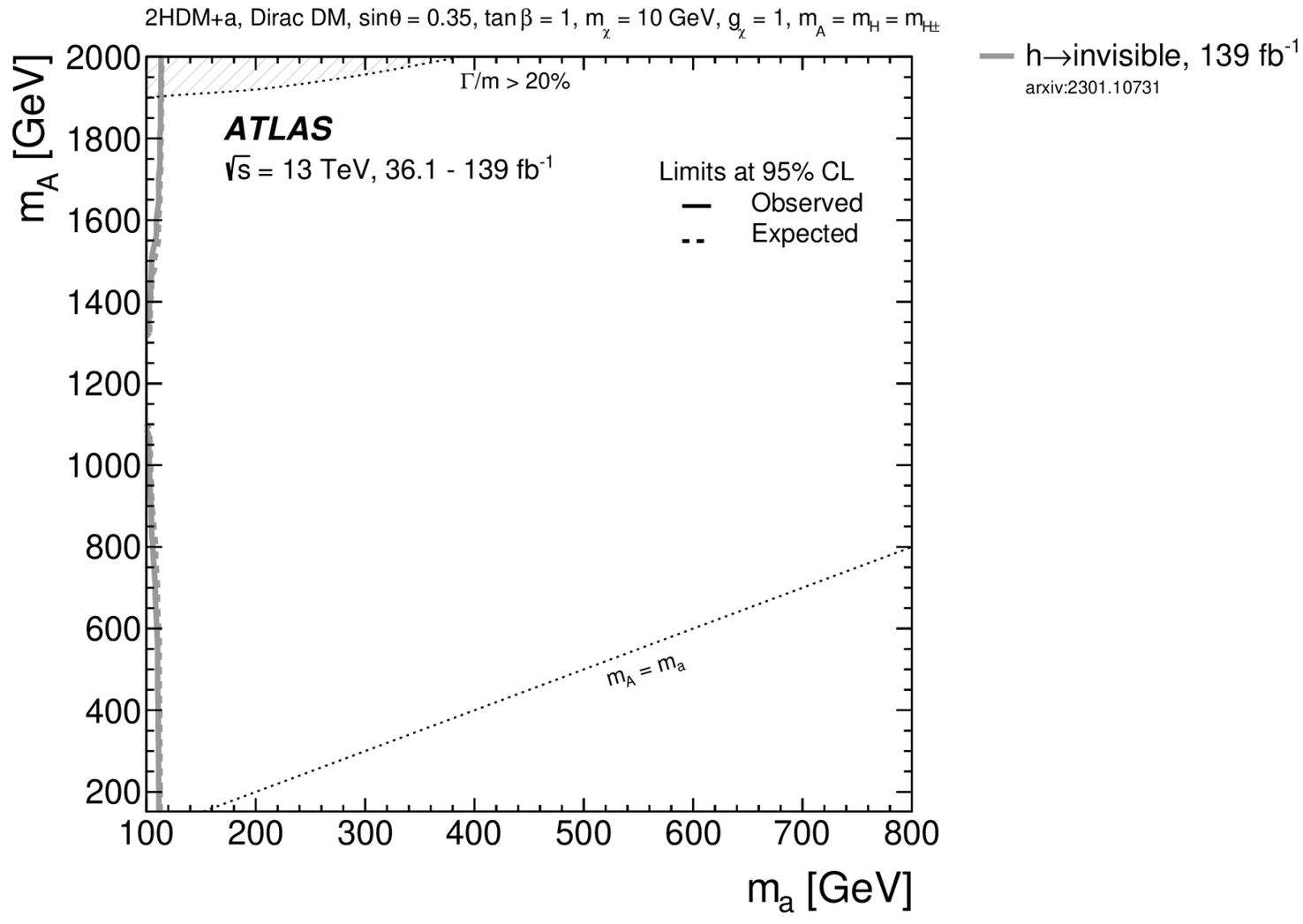

Scenario 1a: $\sin\theta = 0.35$ m_A-m_a plane

- $h \rightarrow$ invisible constrains very low m_a.

- constraints from $E_{\mathrm{T}}^{\mathrm{miss}} + h$ signatures: similar m_A-m_a dependence, with $h \rightarrow bb$ most sensitive.

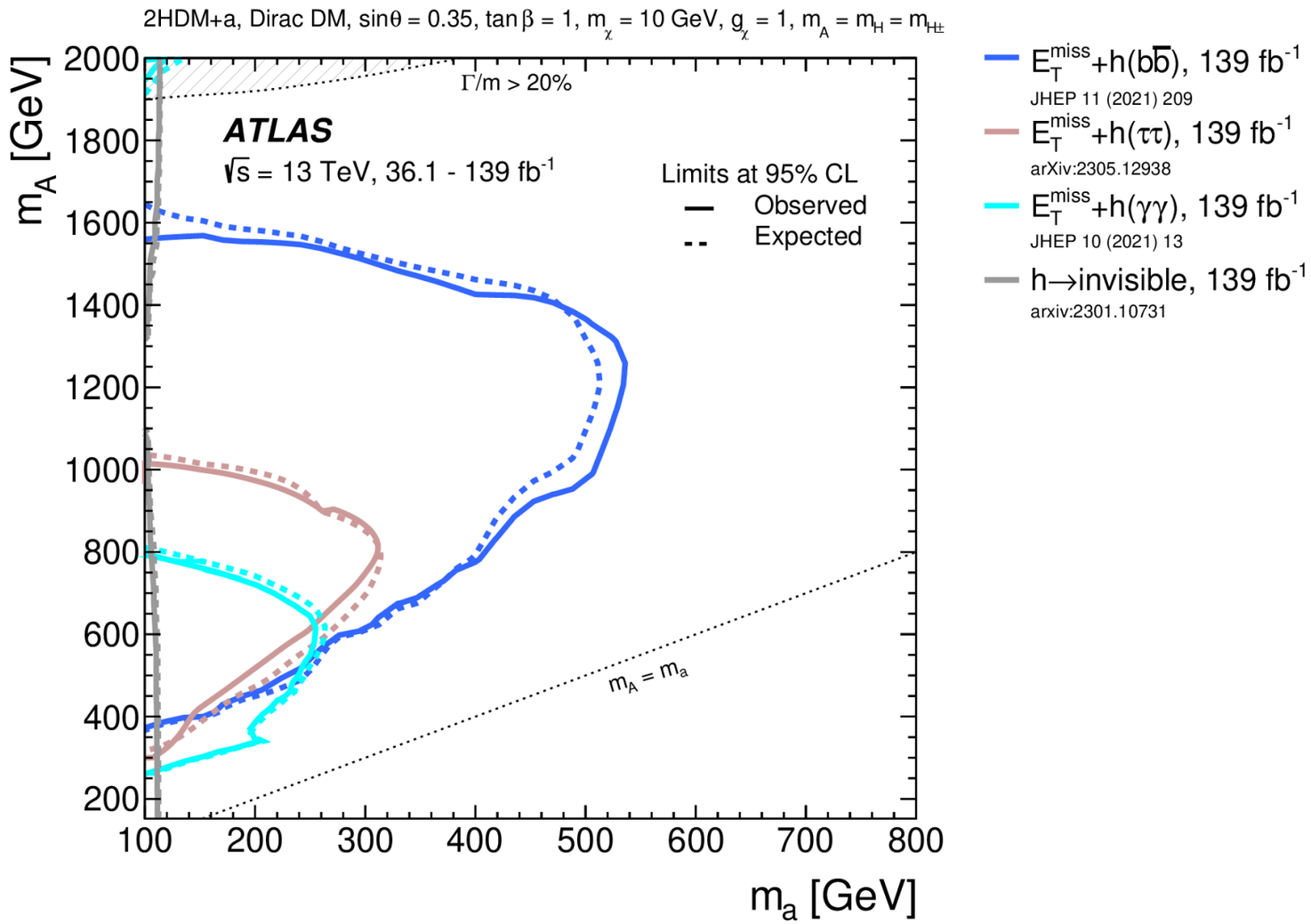

Scenario 1a: $\sin\theta = 0.35$ m_A-m_a plane

- $h \rightarrow$ invisible constrains very low m_a.

- constraints from $E_{\mathrm{T}}^{\mathrm{miss}} + h$ signatures: similar m_A-m_a dependence, with $h \rightarrow bb$ most sensitive.

- $E_{\mathrm{T}}^{\mathrm{miss}} + tW$ similar to $E_{\mathrm{T}}^{\mathrm{miss}} + Z(ll)$ but with smaller excl. region.

- $E_{\mathrm{T}}^{\mathrm{miss}} +$ jet sensitivity notably different from those of $E_{\mathrm{T}}^{\mathrm{miss}} + Z$ and $E_{\mathrm{T}}^{\mathrm{miss}} + h$.

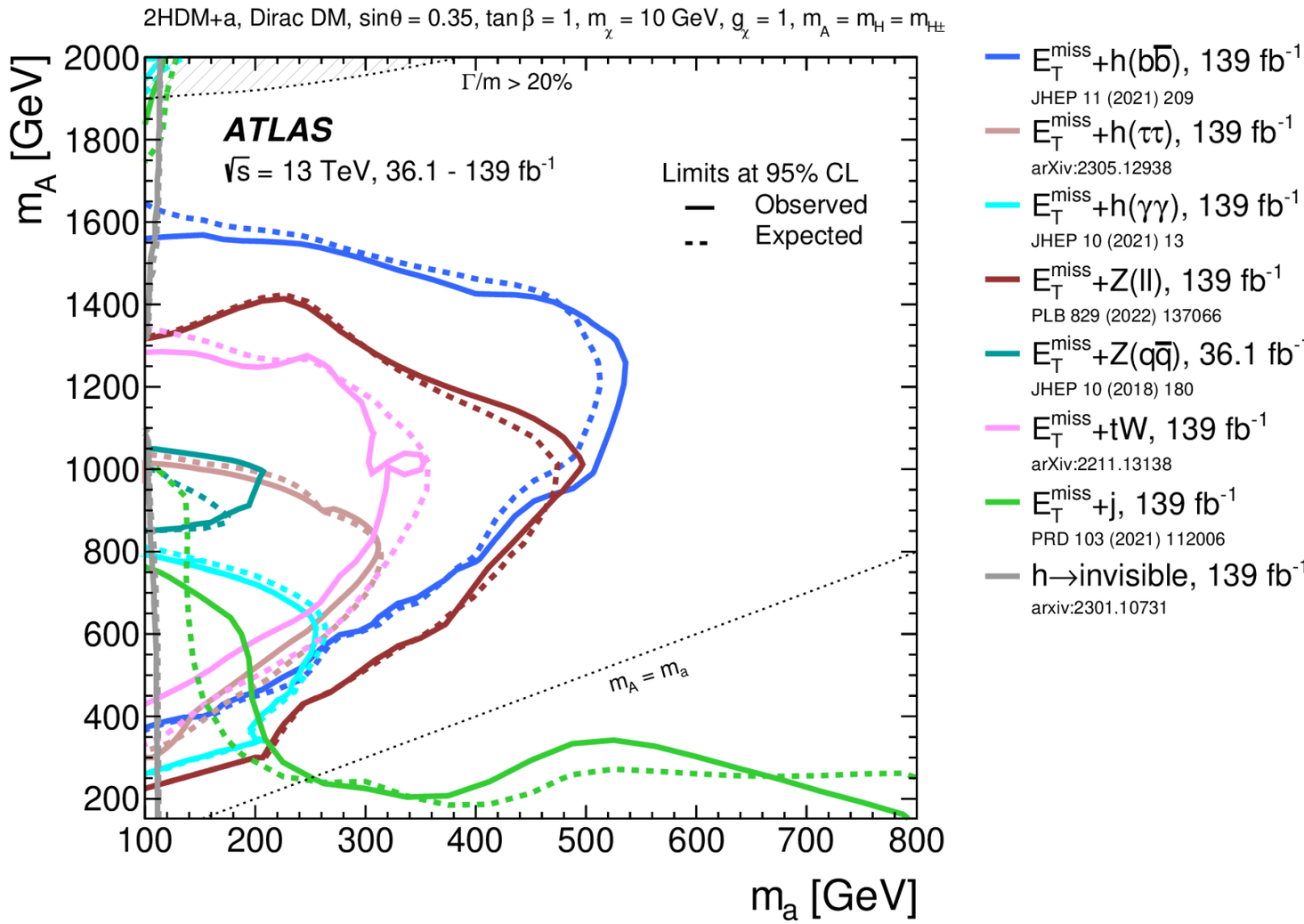

Scenario 1a: $\sin\theta = 0.35$ m_A-m_a plane

- $h \rightarrow$ invisible constrains very low m_a.

- constraints from $E_{\mathrm{T}}^{\mathrm{miss}} + h$ signatures: similar m_A-m_a dependence, with $h \rightarrow bb$ most sensitive.

- $E_{\mathrm{T}}^{\mathrm{miss}} + tW$ similar to $E_{\mathrm{T}}^{\mathrm{miss}} + Z(ll)$ but with smaller excl. region.

- $E_{\mathrm{T}}^{\mathrm{miss}} +$ jet sensitivity notably different from those of $E_{\mathrm{T}}^{\mathrm{miss}} + Z$ and $E_{\mathrm{T}}^{\mathrm{miss}} + h$.

- Complementary constraints from searches not targeting DM.

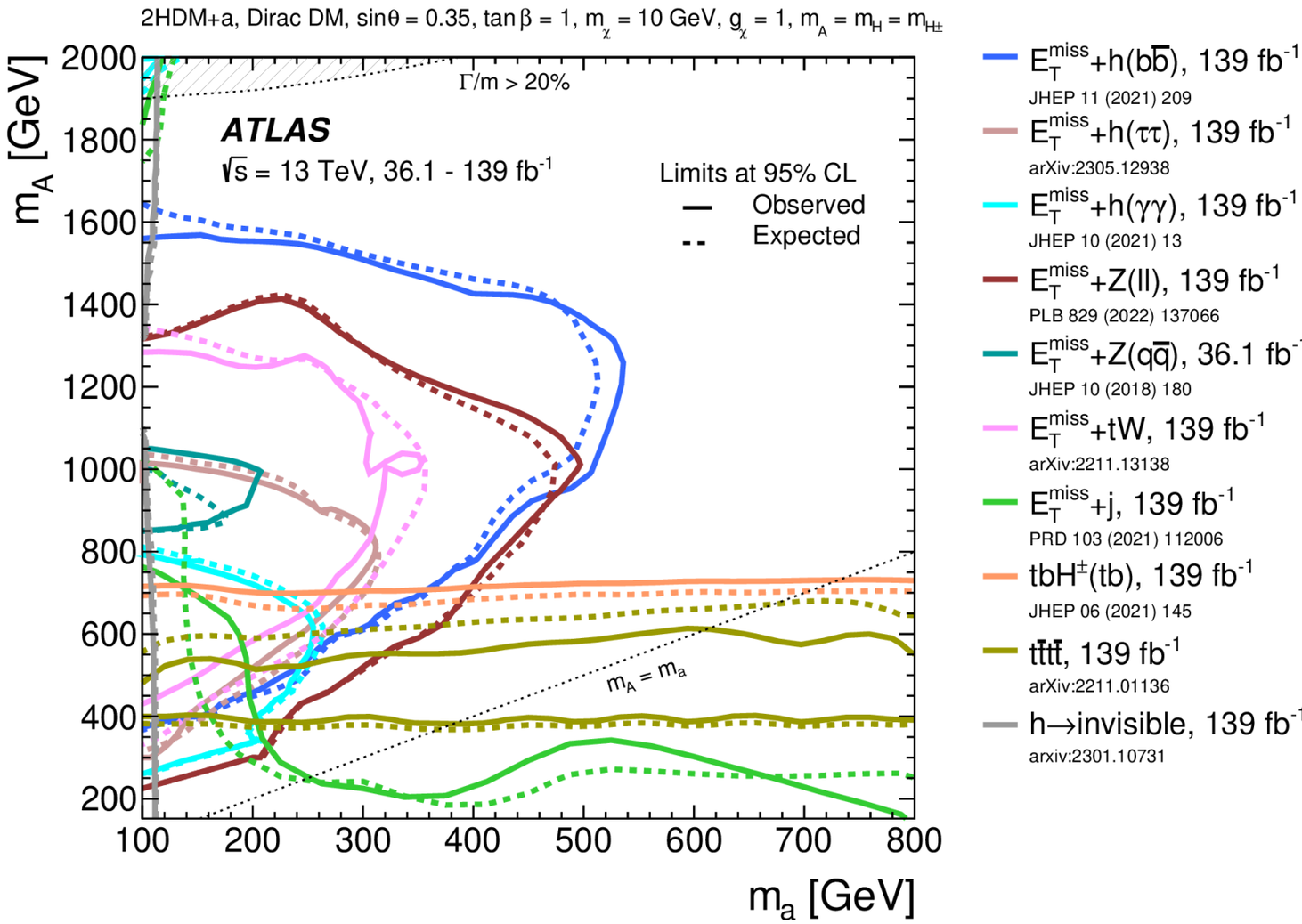

Scenario 1a: $\sin\theta = 0.35$ m_A-m_a plane

- $h \rightarrow$ invisible constrains very low m_a.

- constraints from $E_{\mathrm{T}}^{\mathrm{miss}} + h$ signatures: similar m_A-m_a dependence, with $h \rightarrow bb$ most sensitive.

- $E_{\mathrm{T}}^{\mathrm{miss}} + tW$ similar to $E_{\mathrm{T}}^{\mathrm{miss}} + Z(ll)$ but with smaller excl. region.

- $E_{\mathrm{T}}^{\mathrm{miss}} +$ jet sensitivity notably different from those of $E_{\mathrm{T}}^{\mathrm{miss}} + Z$ and $E_{\mathrm{T}}^{\mathrm{miss}} + h$.

- Complementary constraints from searches not targeting DM.

- Sensitivity of 2HDM+a driven by the combination.

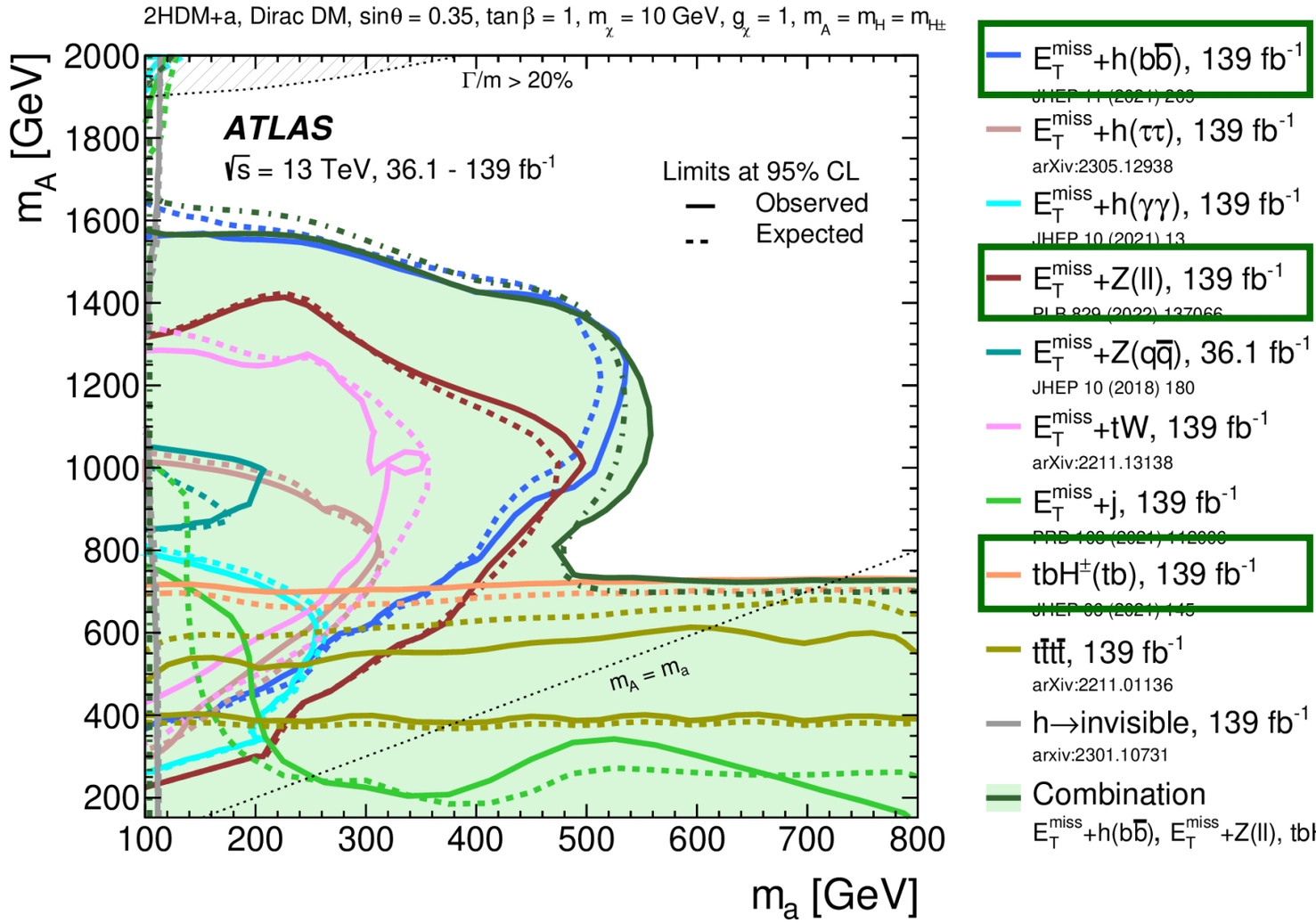

Most comprehensive set of constraints on 2HDM+a to date

Scenario 6: m_a-m_χ plane

- New interpretation in m_a-m_χ plane:
  - Searches for SM Higgs decaying to 4 fermions via aa constrain previously unprobed region of 2HDM+a.
  - Complementarity to $h \rightarrow$ invisible and $E_{\mathrm{T}}^{\mathrm{miss}} + h(bb)$ searches.

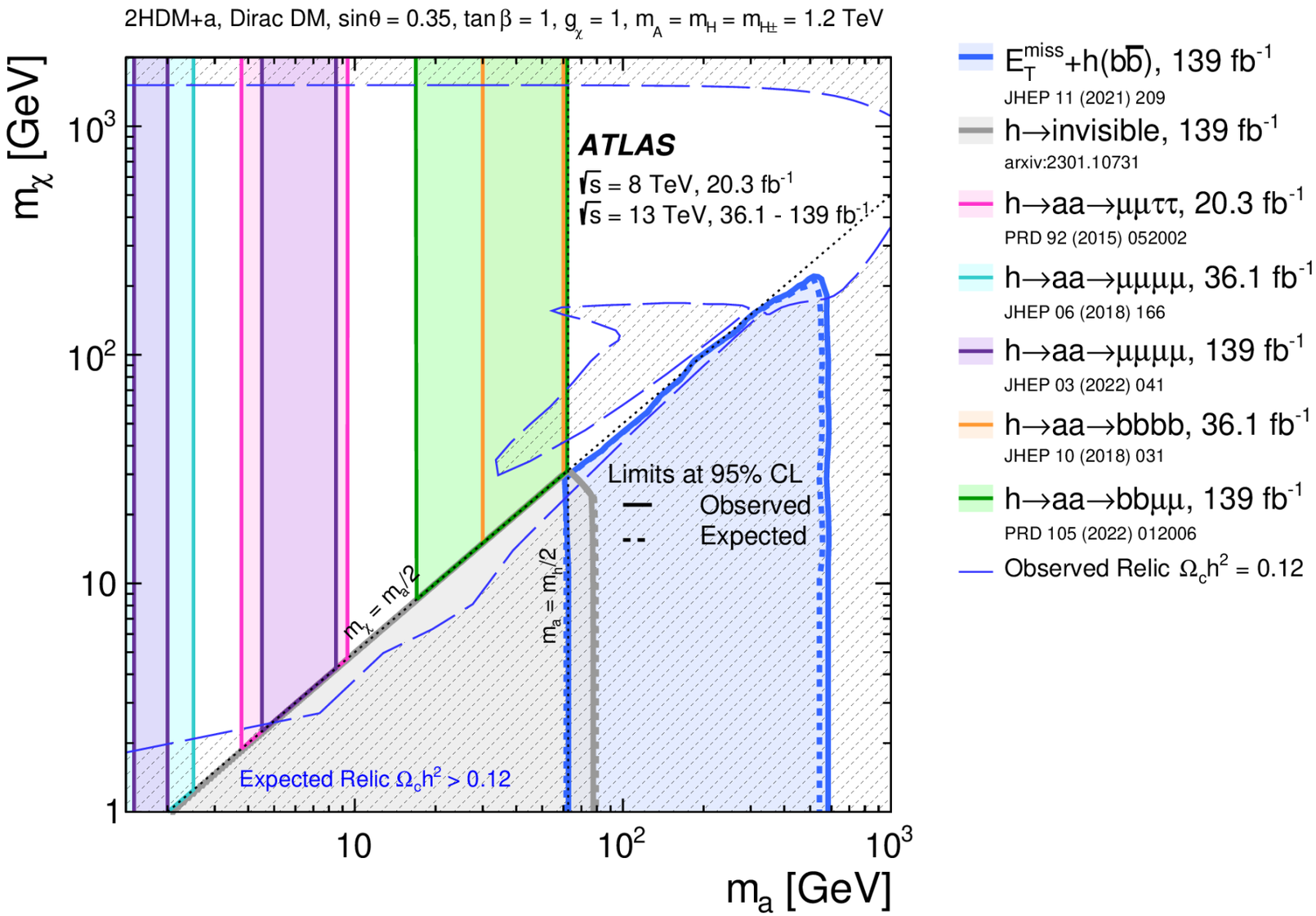

Conclusion

- The results in this paper represent the most comprehensive set of constraints on the 2HDM+a obtained by the ATLAS Collaboration to date. We have determined the sensitivity of many relevant signatures, determining the exclusions of these channels for the first time.

- Statistical combination of $E_T^{miss} + Z(ll)$, $E_T^{miss} + h(bb)$ and $tbH^{\pm}(tb)$ extends the sensitivity to the 2HDM+a compared to the sensitivities derived from the individual searches across different regions of the 2HDM+a parameter space

- For the first time the results of searches targeting $h \to aa \to 4f$ are used to constrain a part of previously unprobed 2HDM+a parameter space.

Thank you for your attention!!!

Backup

2HDM+a

- Coupling of pseudo scalar P to the dark Dirac fermion χ

$$\mathcal{L}_\chi = -iy_\chi P \bar{\chi}\gamma_5\chi\,,$$

- Yukawa couplings of Higgs doublets to SM fermions

$$\mathcal{L}_Y = -\sum_{i=1,2}\left(\bar{Q}Y_u^i\tilde{H}_i u_R + \bar{Q}Y_d^i H_i d_R + \bar{L}Y_\ell^i H_i \ell_R + \text{h.c.}\right)\,.$$

- Most general scalar potential of two Higgs doublets

$$V = V_H + V_{HP} + V_P\,,$$

$$\begin{aligned} V_H = {} & \mu_1 H_1^\dagger H_1 + \mu_2 H_2^\dagger H_2 + \left(\mu_3 H_1^\dagger H_2 + \text{h.c.}\right) + \lambda_1\left(H_1^\dagger H_1\right)^2 + \lambda_2\left(H_2^\dagger H_2\right)^2 \\ & + \lambda_3\left(H_1^\dagger H_1\right)\left(H_2^\dagger H_2\right) + \lambda_4\left(H_1^\dagger H_2\right)\left(H_2^\dagger H_1\right) + \left[\lambda_5\left(H_1^\dagger H_2\right)^2 + \text{h.c.}\right]\,, \end{aligned}$$

$$V_{HP} = P\left(ib_P H_1^\dagger H_2 + \text{h.c.}\right) + P^2\left(\lambda_{P1} H_1^\dagger H_1 + \lambda_{P2} H_2^\dagger H_2\right)\,,$$

$$V_P = \frac{1}{2}m_P^2 P^2\,.$$

$E_{\mathrm{T}}^{\mathrm{miss}} + tW$ signature

(0- and 1-lepton) Eur. Phys. J. C 83 (2023) 603

(2-lepton) Eur. Phys. J. C 81 (2021) 860

- optimised specifically for 2HDM+a and particularly sensitive to on-shell $H^{\pm} \to W^{\pm}a(\chi\bar{\chi})$
- Final interpretations
  - include both 2HDM+a $E_{\mathrm{T}}^{\mathrm{miss}} + t\bar{t}$ and $E_{\mathrm{T}}^{\mathrm{miss}} + tW$ signal contributions.
  - with combination of all three 0-, 1-, and 2-lepton channels.

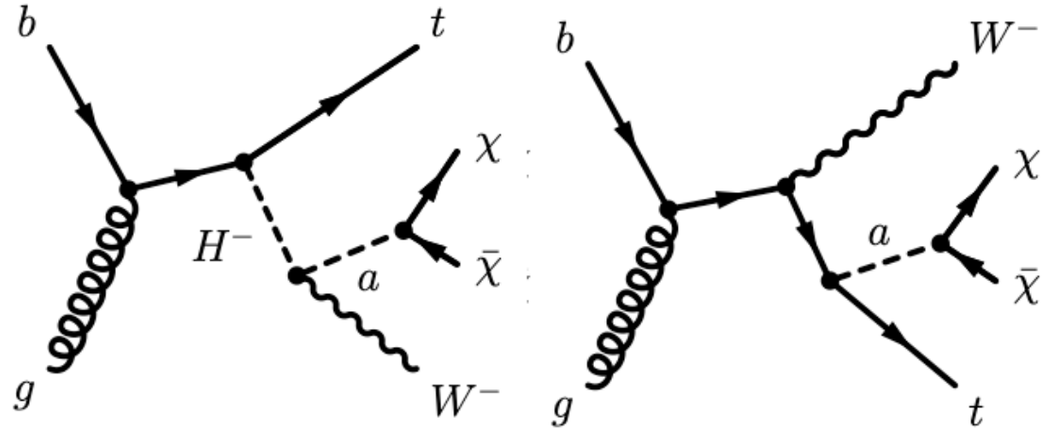

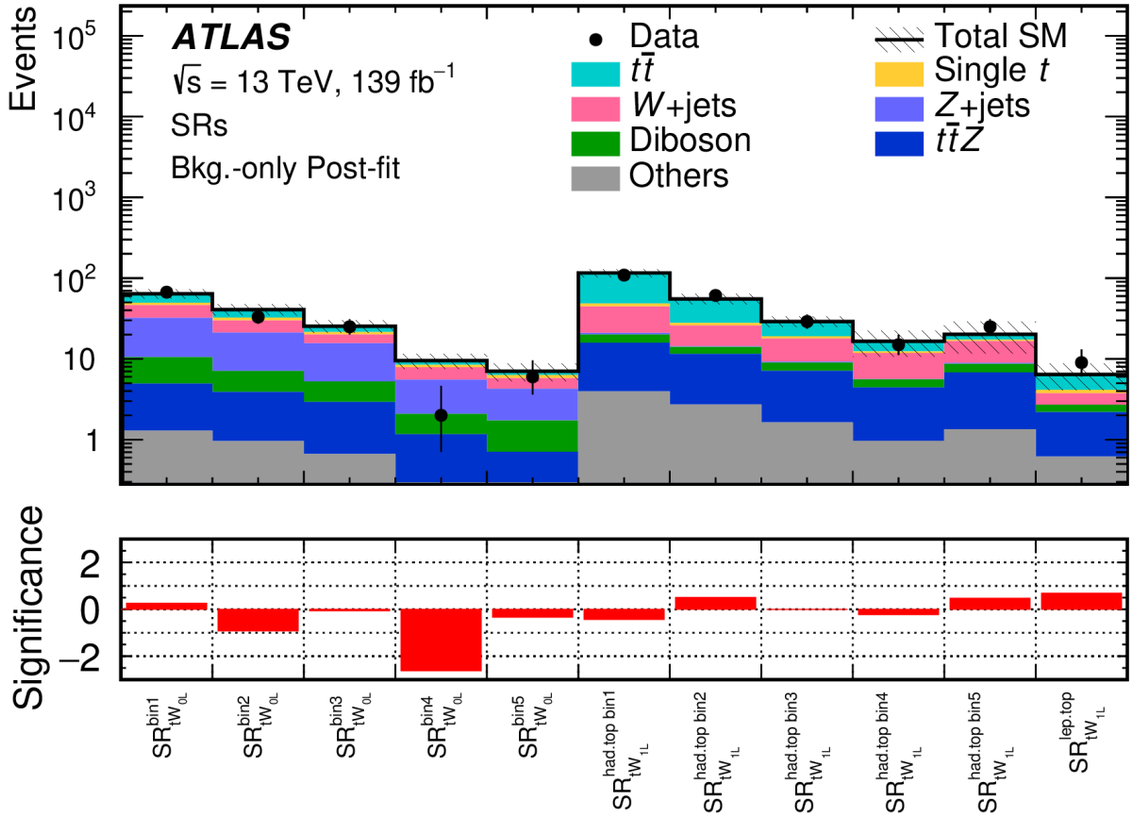

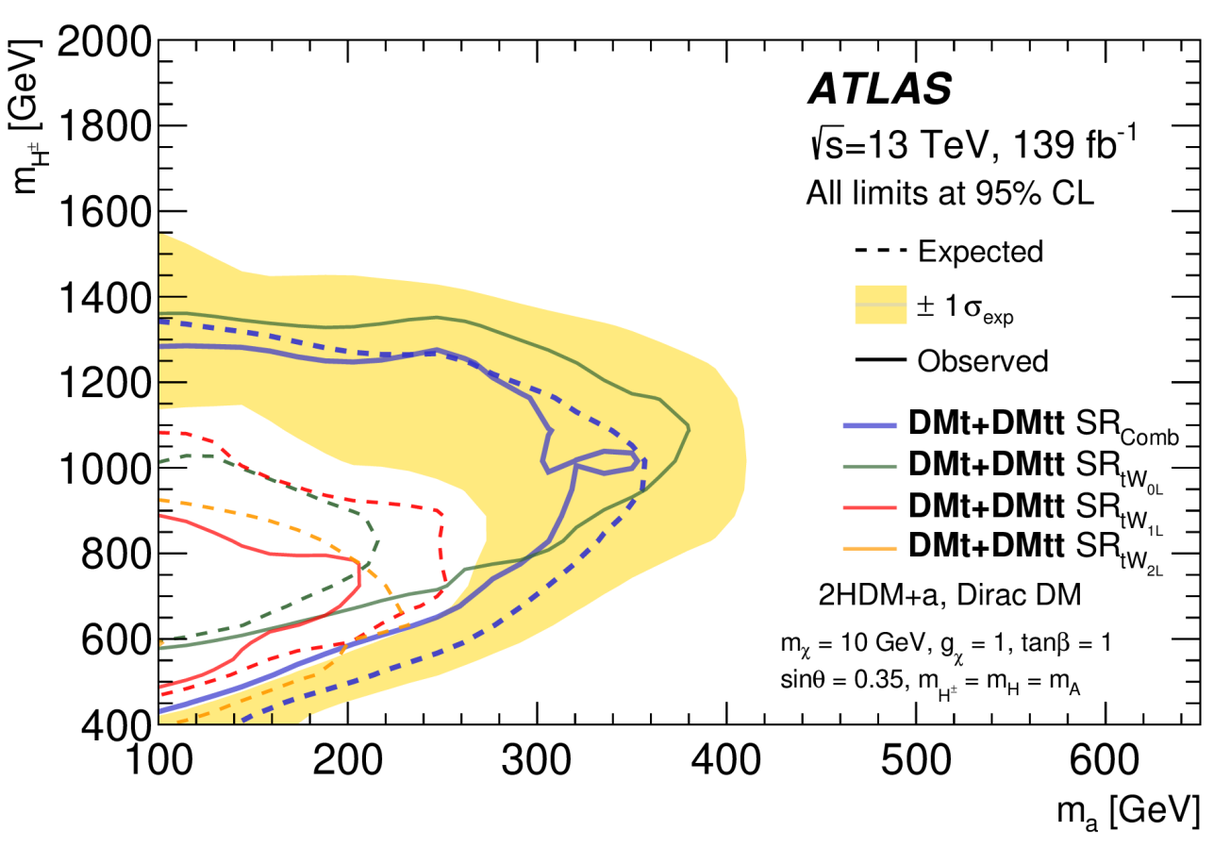

HLRS searches

For lower values of m_a, there is strong complementarity with light resonance searches for H->aa->4f. A m_a —m_χ scan has been designed to illustrate that.

Benchmark model parameters tuned to evade constraints from total Higgs width:

$$\{m_A, \tan\beta, \sin\theta, \lambda_3, y_\chi\} = \{1.2\,\text{TeV}, 1, 0.35, 3, 1\}$$

Results from the following searches are used as inputs for m_a—m_χ scan:

- search for H → aa → bbμμ [arXiv:2110.00313]
- search for H → aa → bbbb [arXiv:1806.07355]
- two searches of the H → XX/ZX → *llll* [arXiv:1802.03388, arXiv:2110.13673]
- search for H → aa → *μμττ*[arXiv:1505.01609]

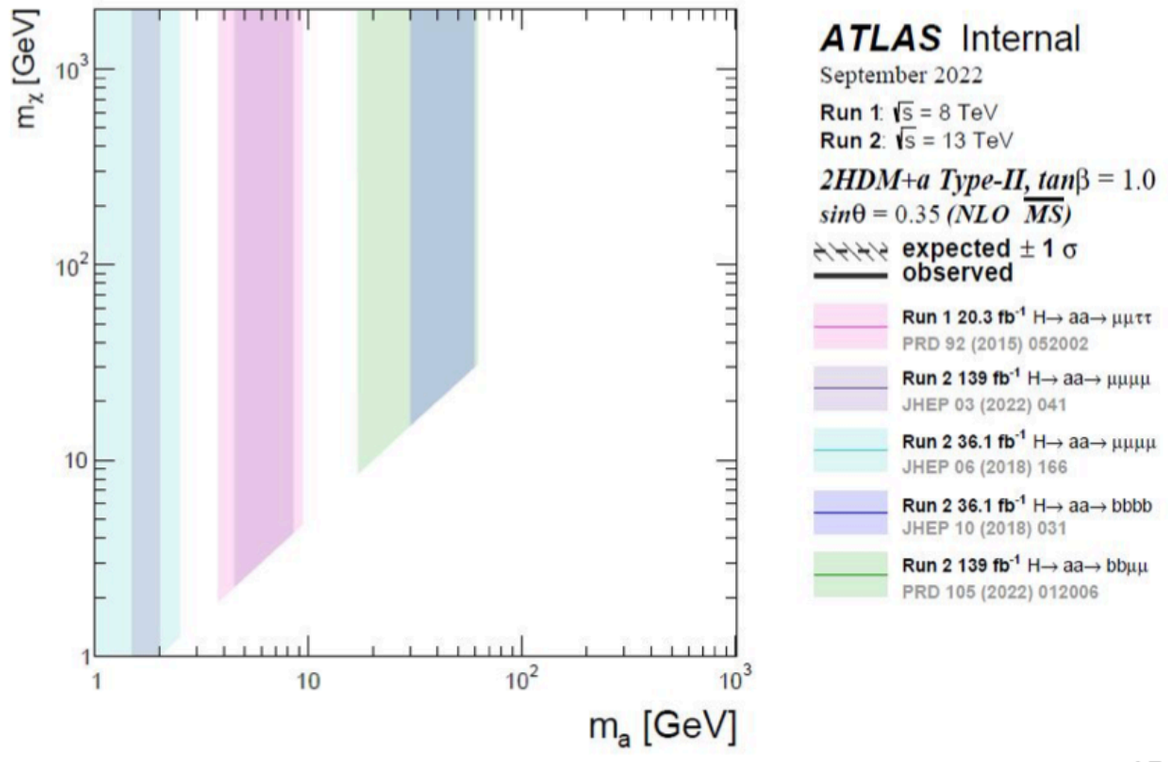

Statistical combination of results

Orthogonality checks

- The statistical combination is facilitated as the input analyses statistically independent.
- Due to b- and lepton-multiplicity requirements, no overlap between the 3 analyses SRs is expected.
- Negligible ($\ll 1\,\%$) event overlap observed between $H^{\pm} \to tb$ SR and $E_T^{miss} + h(bb)$ CR, no impact on the combination.

Input Analysis	Signal selection
EtMiss + Z(ll)	b-jet veto
EtMiss + h(bb)	>= 2 b-jets, 0 lepton
Charged H -> tb	>= 3 b-jets, 1 lepton

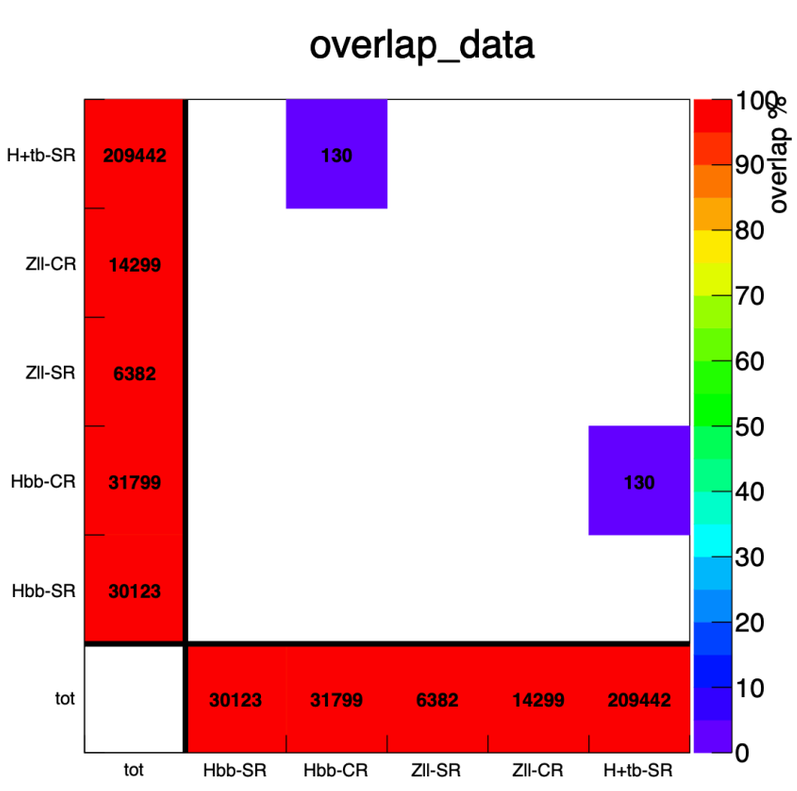

(a) Full run 2 data, number of overlapped events

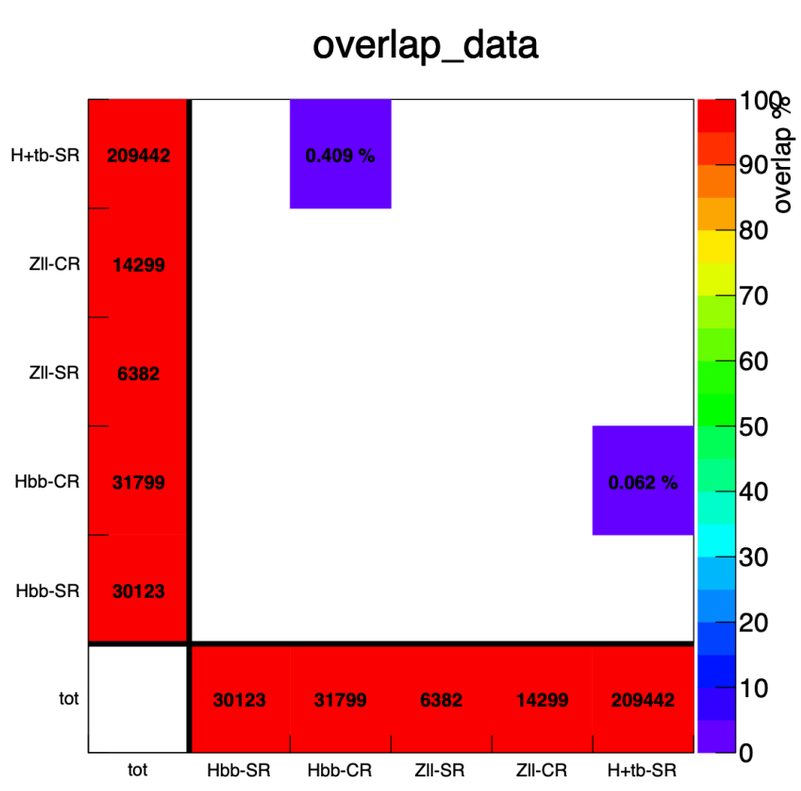

(b) Full run 2 data, fraction of overlapped events

Statistical combination of results

Statistical analysis

- The combination is performed by constructing the analyses' likelihood and maximizing the corresponding profile likelihood ratio.

- The likelihood used in the combination defined as:

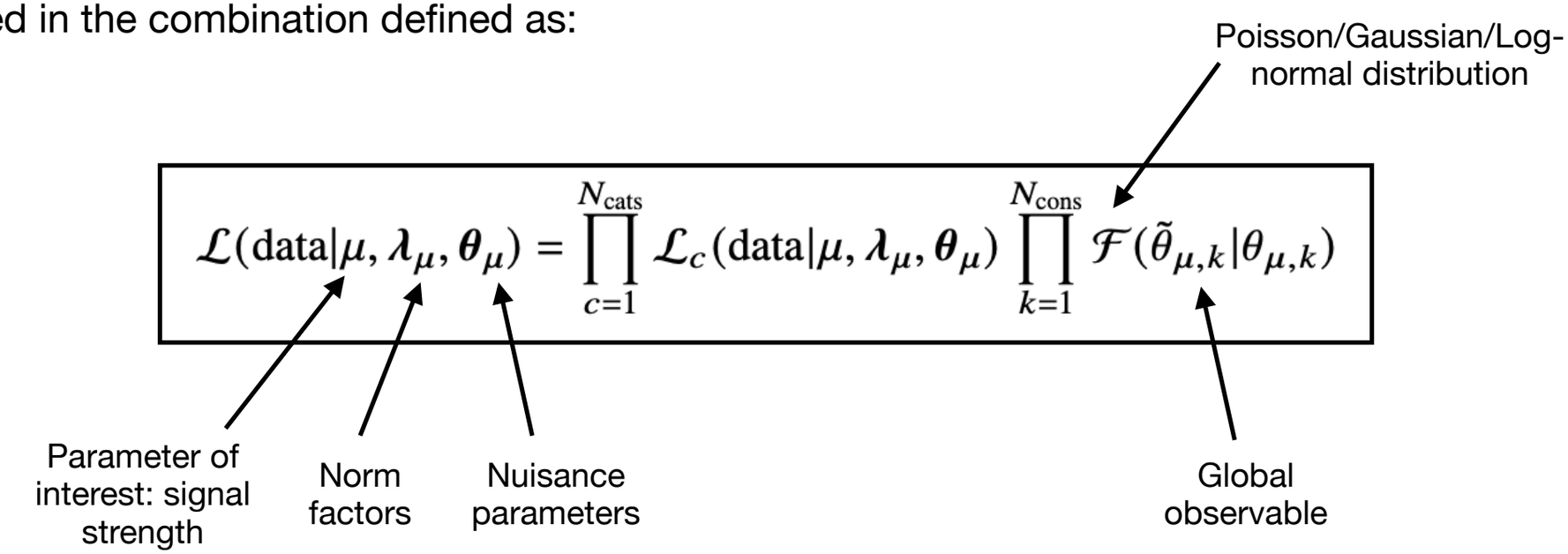

- 95% CL limits are obtained using the profile likelihood ratio test statistic as:

$$q_\mu = \frac{\mathcal{L}(\mu, \hat{\hat{\boldsymbol{\lambda}}}_\mu, \hat{\hat{\boldsymbol{\theta}}}_\mu))}{\mathcal{L}(\hat{\mu}, \hat{\boldsymbol{\lambda}}_{\hat{\mu}}, \hat{\boldsymbol{\theta}}_{\hat{\mu}})},$$

Statistical combination of results

Combination strategy

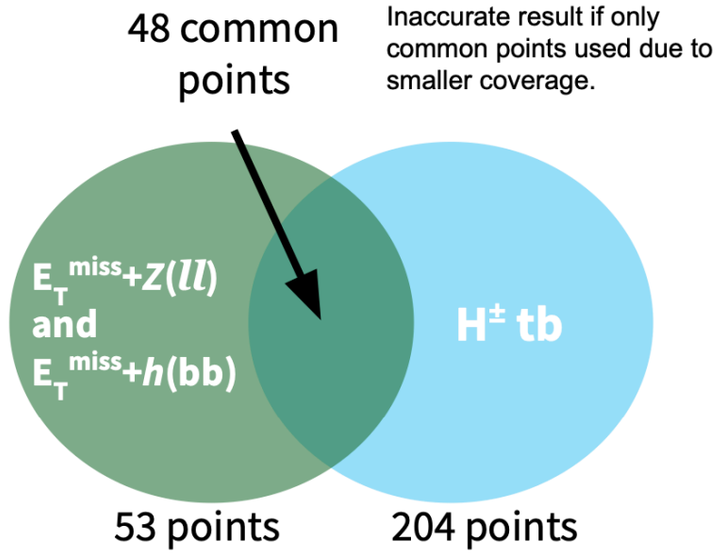

- $tbH^{\pm}(tb)$ added to stat. combination with $E_T^{miss} + Z(ll)$ and $E_T^{miss} + h(bb)$ for the first time → can significantly improve sensitivity.

- Usually, the combination is done for every common signal point over 3 channels.

- Hybrid combination approach: exclude channels that have negligible sensitivities in a certain region.
  - $m_A > 1500$ GeV: $E_T^{miss} + Z(ll)$ and $E_T^{miss} + h(bb)$.
  - $m_A < 1500$ GeV and $m_A > m_a$: all 3 channels combined.
  - $m_A < m_a$ (off-shell region for mono-X searches): $H^{\pm} \to tb$ only.

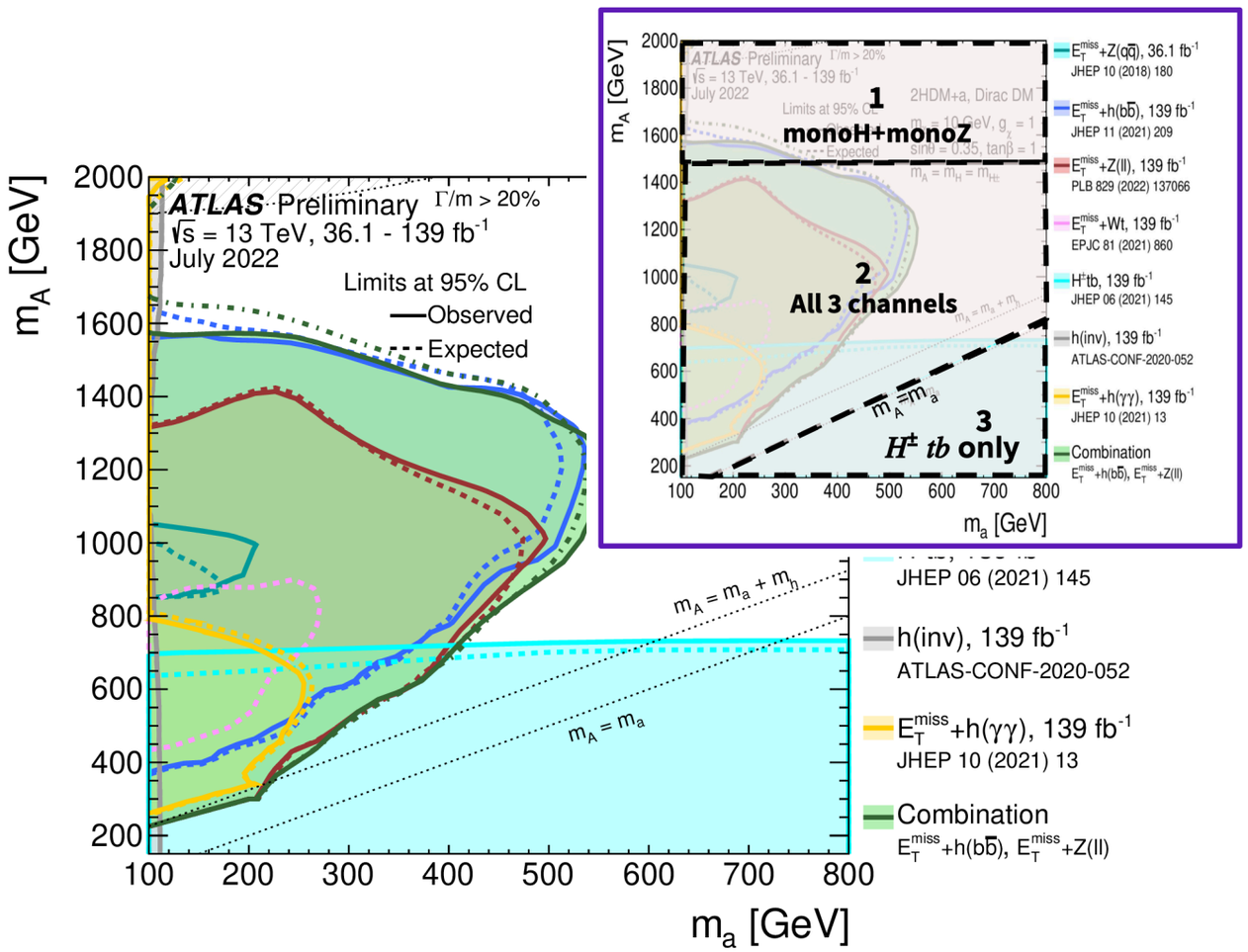

Statistical combination of results

Uncertainties and their correlations

- Most experimental uncertainties related to reconstruction of physics objects are correlated across search channels.
- Uncertainties stemming from b-jet identification are not correlated due to different choices of algorithm and operating point.
- Uncertainties constrained in a particular analysis are not correlated to avoid bringing tensions from any phase-space-specific biases across channels.
- Due to different processes and phase spaces being probed, modelling uncertainties are uncorrelated across analyses.
- Different correlation choices for FTAG/JER/MET and strongly-constrained NPs were tested without observed impact on the exclusions.

Uncertainty source	$\Delta\mu$ [%]
Statistical uncertainty	25.0
Systematic uncertainties	27.6
Theory uncertainties	16.2
Signal modelling	2.8
Background modelling	15.9
Experimental uncertainties (excl. MC stat.)	18.8
Luminosity, pile-up	3.9
Jets, $E_{\mathrm{T}}^{\mathrm{miss}}$	12.3
Flavour tagging	9.1
Electrons, muons	6.1
MC statistical uncertainty	9.3
Total uncertainty	37.2

stat. and syst. uncertainties to tot. uncertainty on the best-fit μ for ($m_a = 450$ GeV, $m_H = 800$ GeV, $\tan\beta = 1$ and $\sin\theta = 0.35$) excluded by the combination but is not by any single input analysis

Statistical combination of results

Uncertainties and their correlations

Correlation Scheme

Correlation scheme is studied and developed based on signal at m_A=800, m_a=500, tanβ= 1 and sinθ=0.35, in the "intersection" region where it has not been excluded in all three channels but within the reach of sensitivity from combination.

NP rankings for single channels could be reproduced.

The majority of leading NPs are channel-specific systematics (e.g., theory systematics on the background modeling). The impact from correlation should be small.

$E_T^{miss}+h(bb)$

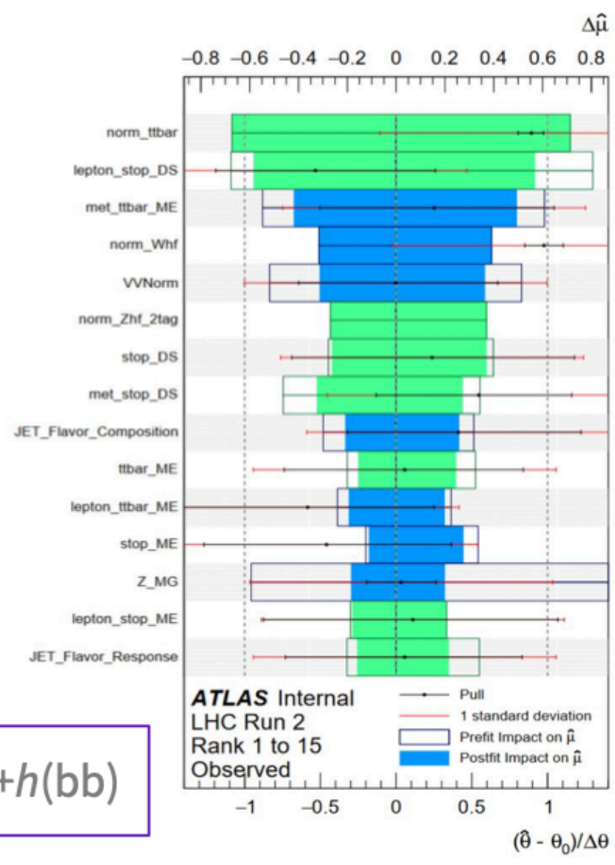

$E_T^{miss}+Z(ll)$

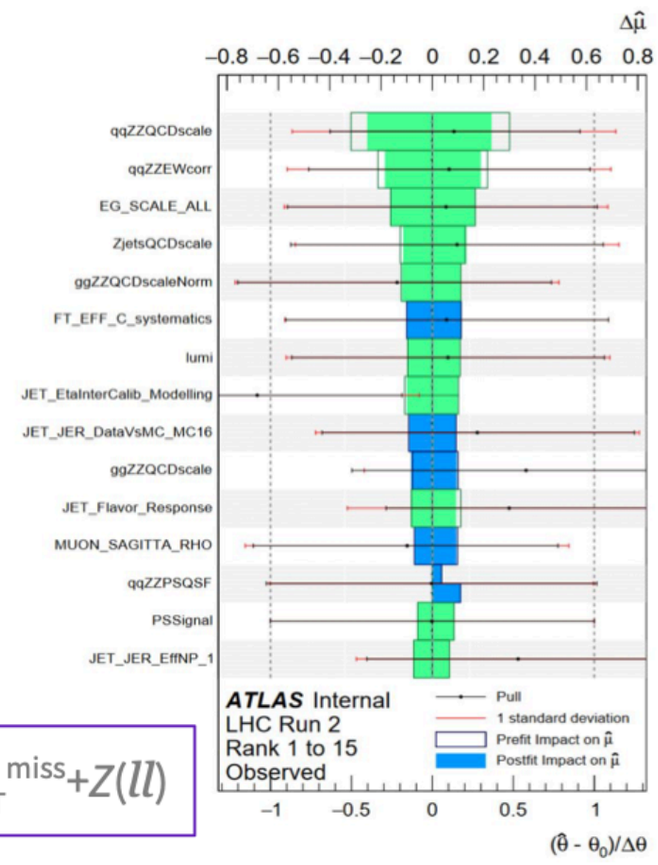

$H^{\pm}$ tb

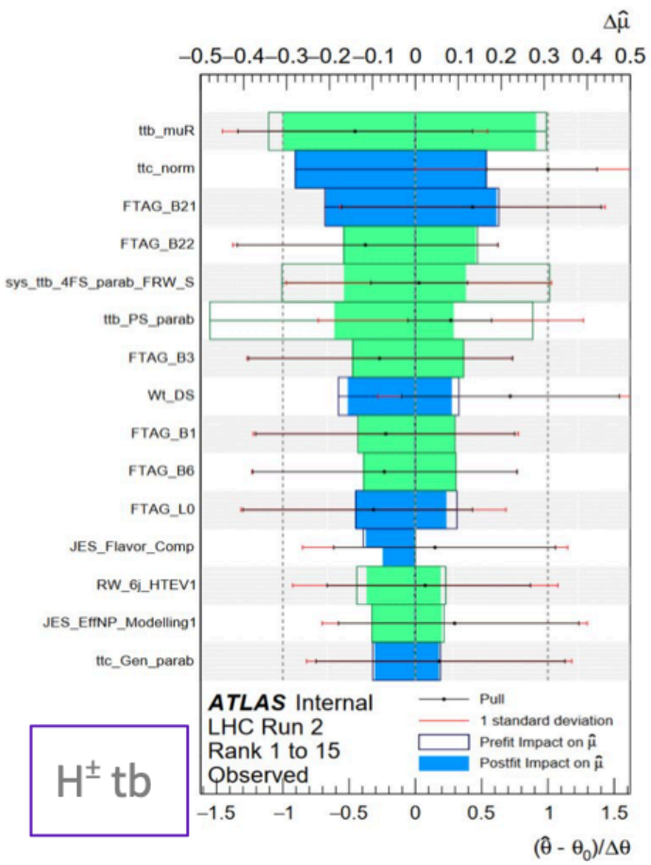

Scenario 1b: $\sin\theta = 0.7$ m_A-m_a plane

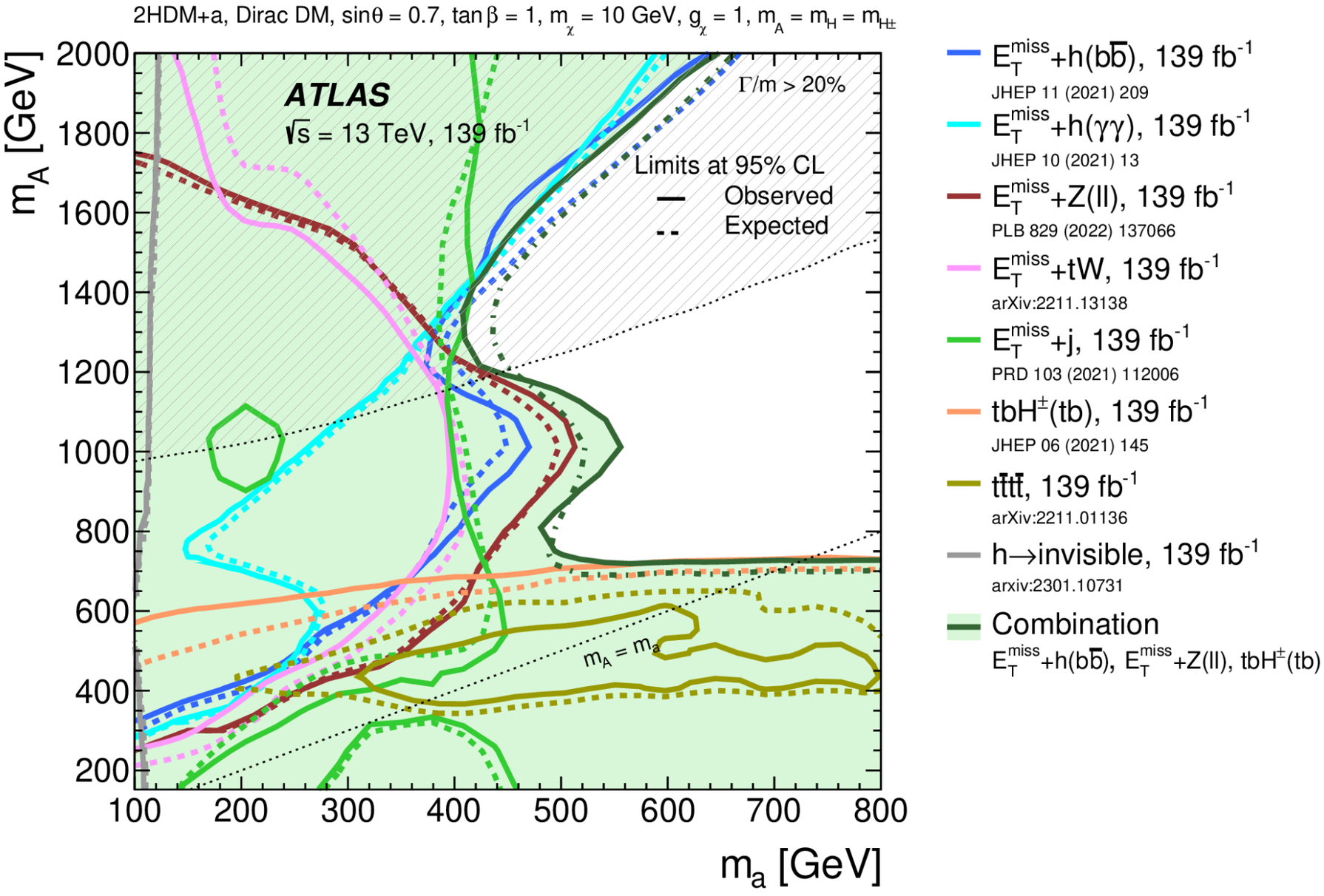

Scenario 2: $m_A - \tan\beta$ planes

- Large fraction of parameter plane excluded by $E_T^{miss} + Z(ll)$, $E_T^{miss} + h(bb)$ dominates in high-m_A but still gives sensitivity in low-m_A with $tbH^{\pm}(tb)$.
- $E_T^{miss} + Z(ll)$ and $E_T^{miss} + h(bb)$ sensitivities driven by the transition from gg- to bb-initiated production with a decrease at $\tan\beta \approx 5$.
- Combination significantly improves the excl. parameter space.

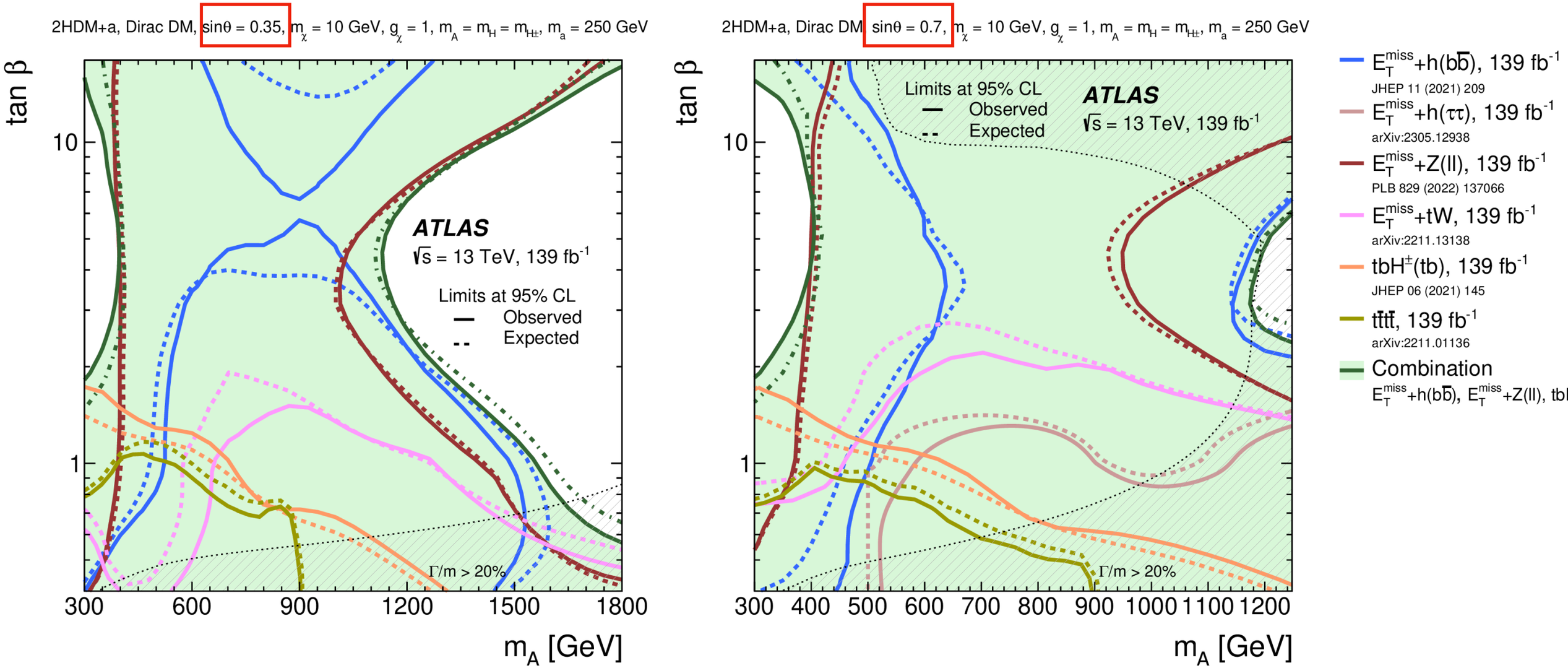

Scenario 3: $m_a - \tan\beta$ planes

- Strongest exclusion from $E_T^{miss} + Z(ll)$, $tbH^{\pm}(tb)$ is complementary to low-$\tan\beta$ region and moderate dependence on m_a.
- Significant improvement in sensitivity achieved by combination.

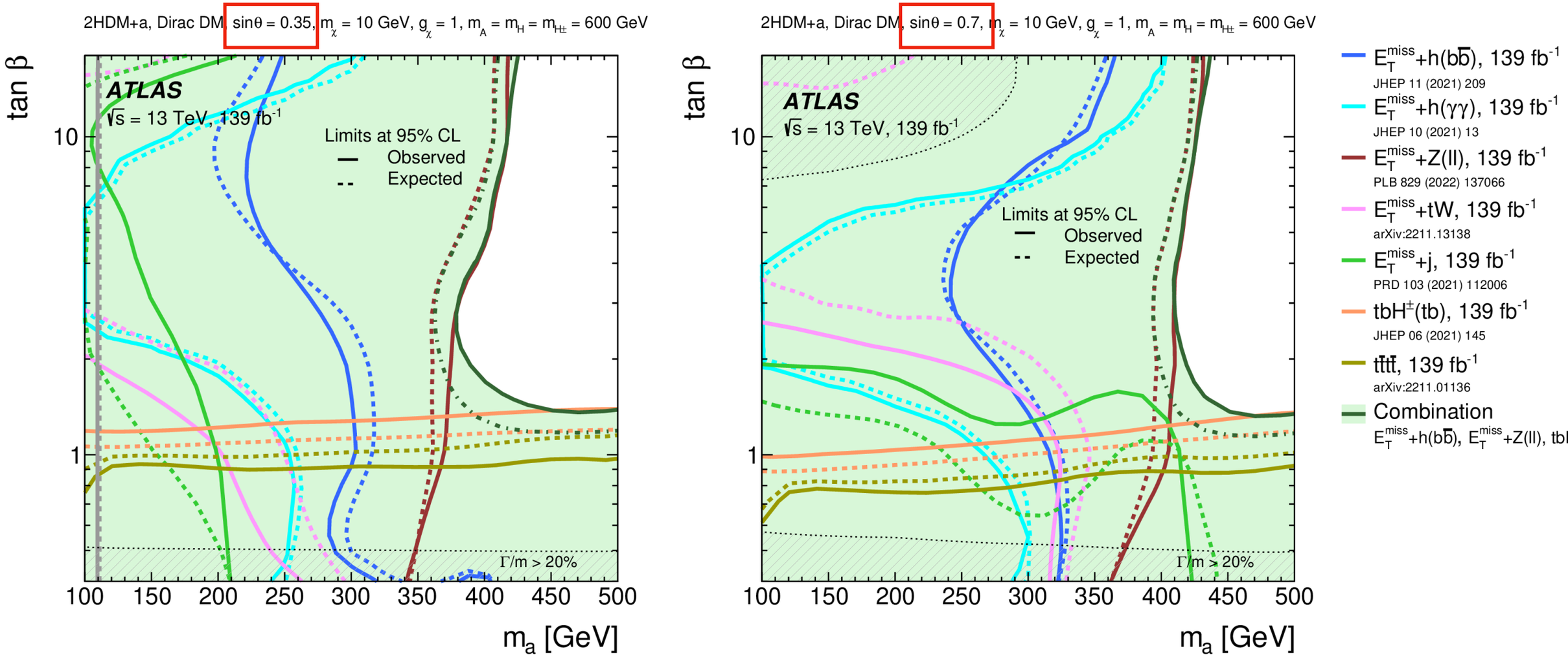

Scenario 4: $\sin\theta$ scans

- $E_T^{miss} + Z(ll)$ and $E_T^{miss} + h(bb)$ provide strongest limits.

- Significant improvement from combination, almost the whole range excluded for these two benchmarks.

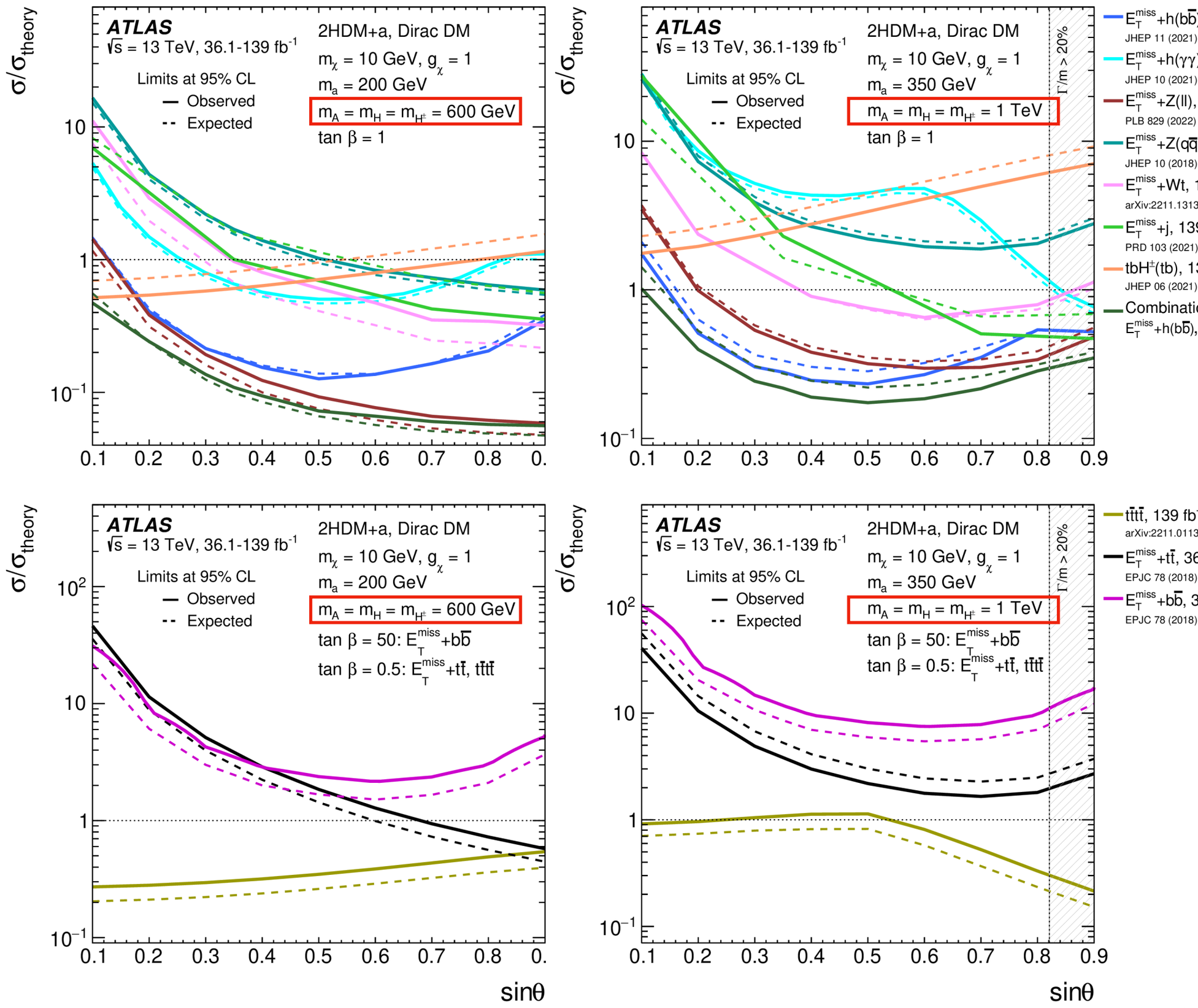

Scenario 5: m_χ scan

- At low-m_χ ($m_\chi < m_a/2$) sensitivity is driven by $E_T^{miss} + Z(ll)$ and $E_T^{miss} + h(bb)$ as the pseudoscalar is allowed to decay in to $\chi\chi$.

- For higher DM masses ($m_\chi > m_a/2$), the sensitivity of $E_T^{miss} + X$ decreases rapidly, while that of $tbH^{\pm}(tb)$ and 4top remains nearly constant. Although none of them excludes 2HDM+a.

- Combination provides strongest exclusion.

- Possible to match the observed relic density for $m_\chi \approx 170$ GeV without changing the collider phenomenology.

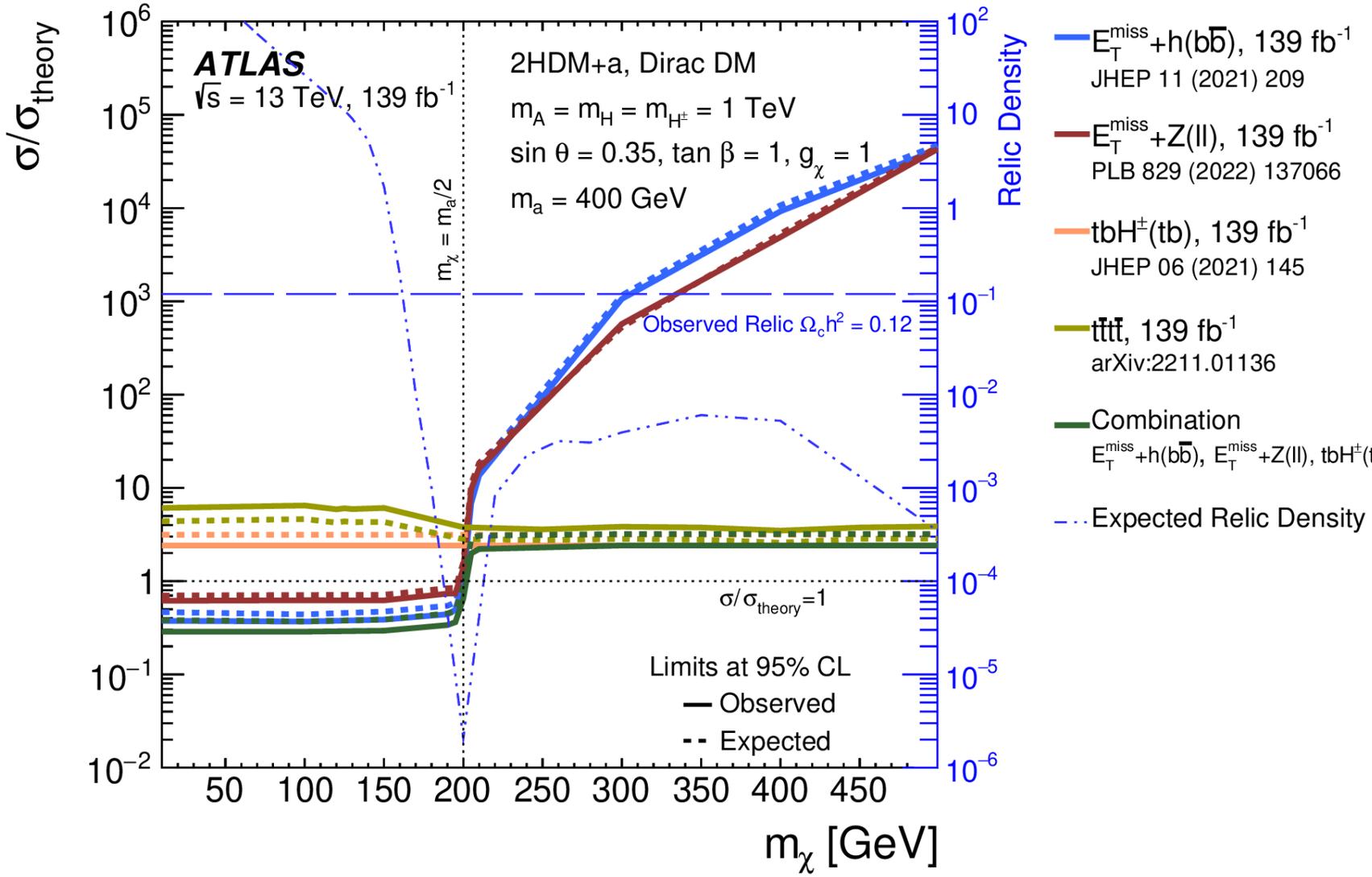

VBF $H \to \gamma\gamma_d$

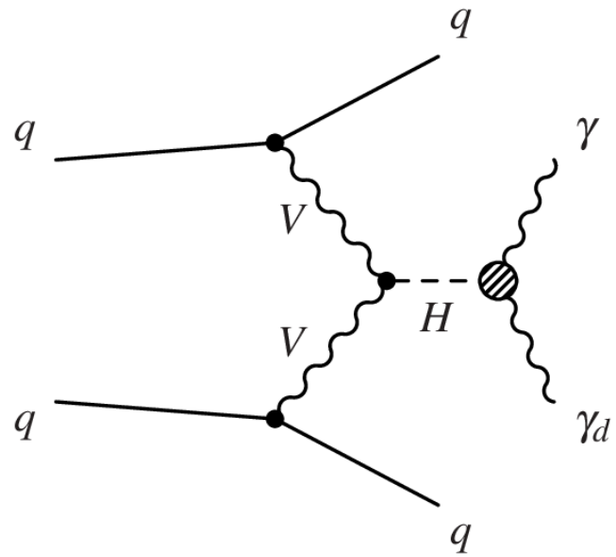

Eur. Phys. J. C 82 (2022) 105

- search for $H \to \gamma\gamma_d$ with VBF production mode
  - $m_H \in [60,2000]$ GeV; massless dark photon;
  - dark photon collider stable → $E_{\mathrm{T}}^{\mathrm{miss}}$;
  - final state with 1 photon, jets and $E_{\mathrm{T}}^{\mathrm{miss}}$.
- Signal region: single-photon trigger, isolated photon, 2 forward jets with $\Delta\eta_{jj} > 2.5$, high $E_{\mathrm{T}}^{\mathrm{miss}}$.
- SR and CRs divided into 2 bins of m_{jj} with 5 bins of $m_T(\gamma, E_{\mathrm{T}}^{\mathrm{miss}})$ each.
- ggF $H \to \gamma\gamma_d$ signal contribution included for 125 GeV Higgs.

An observed (expected) 95% CL upper limit on the branching ratio for this decay is set at 0.018 ($0.017^{+0.007}_{-0.005}$), assuming the SM 125 GeV Higgs boson.

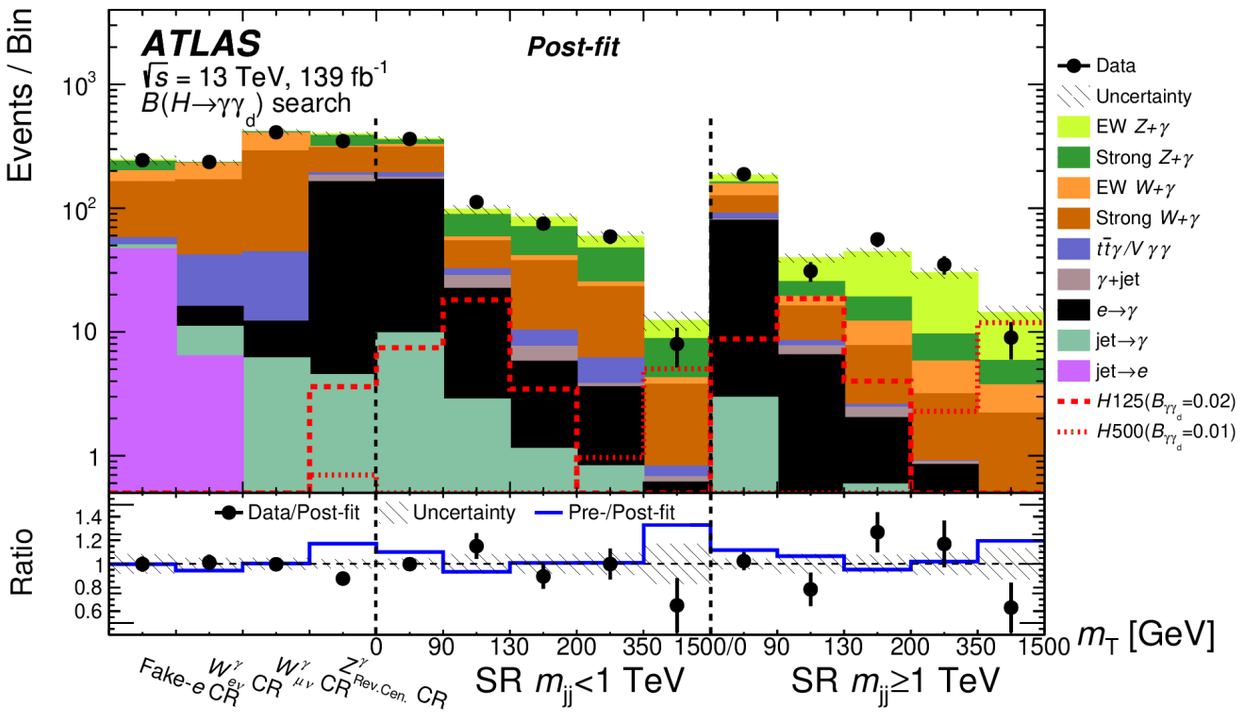

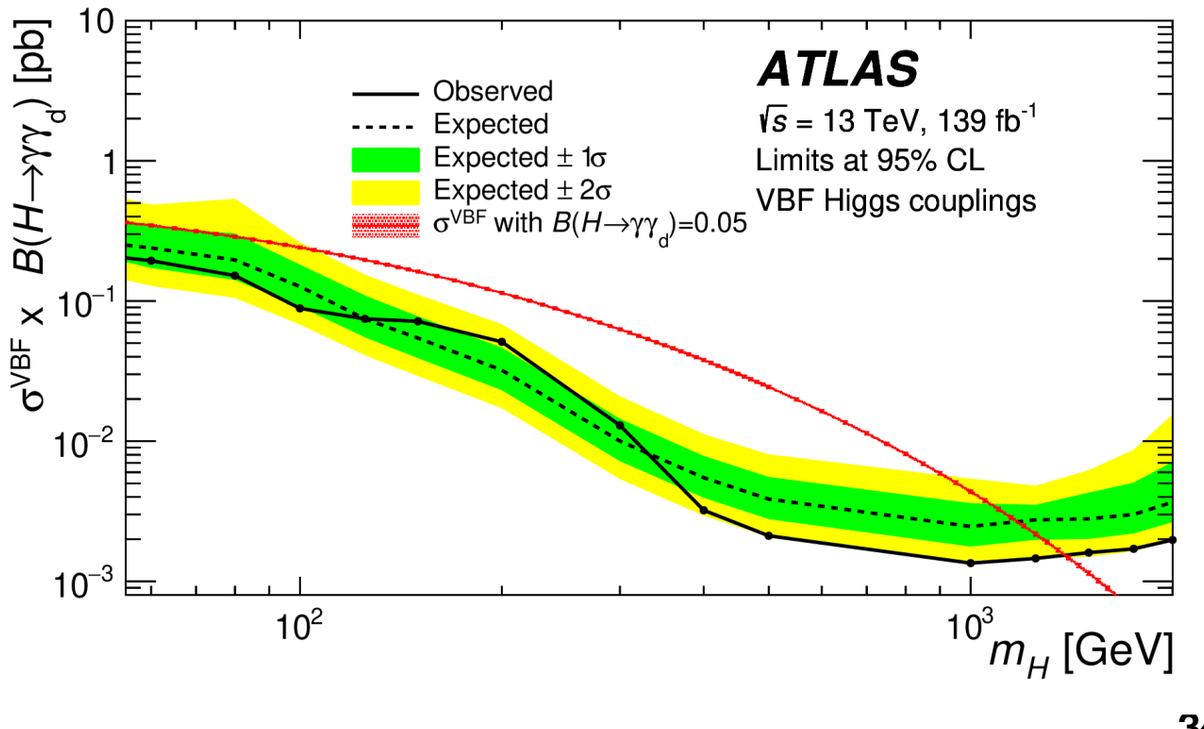

$ZH, H \to \gamma\gamma_d$

JHEP 07 (2023) 133

- Search for $H \to \gamma\gamma_d$ with ZH production mode
  - m_H = 125 GeV; $m_{\gamma_d} \in [0,40]$ GeV;
  - dark photon → $E_{\mathrm{T}}^{\mathrm{miss}}$; $Z \to l^+l^-$;

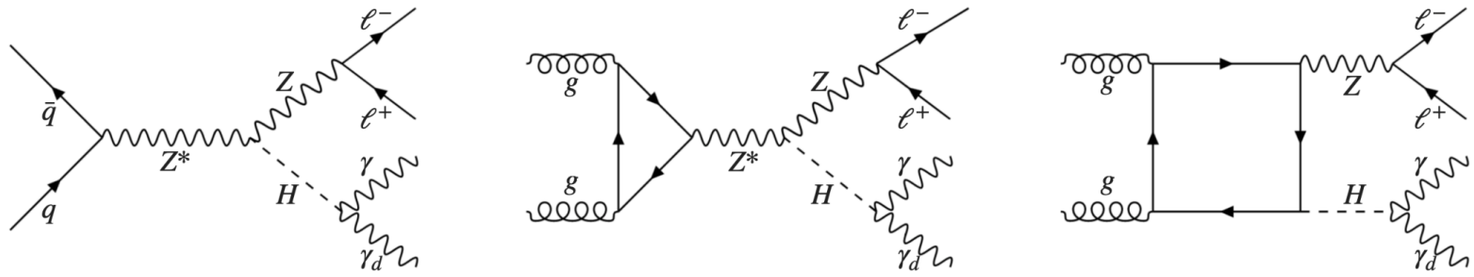

- BDT (XGBOOST) optimised specifically for 125 GeV Higgs, used to enhance sensitivity.

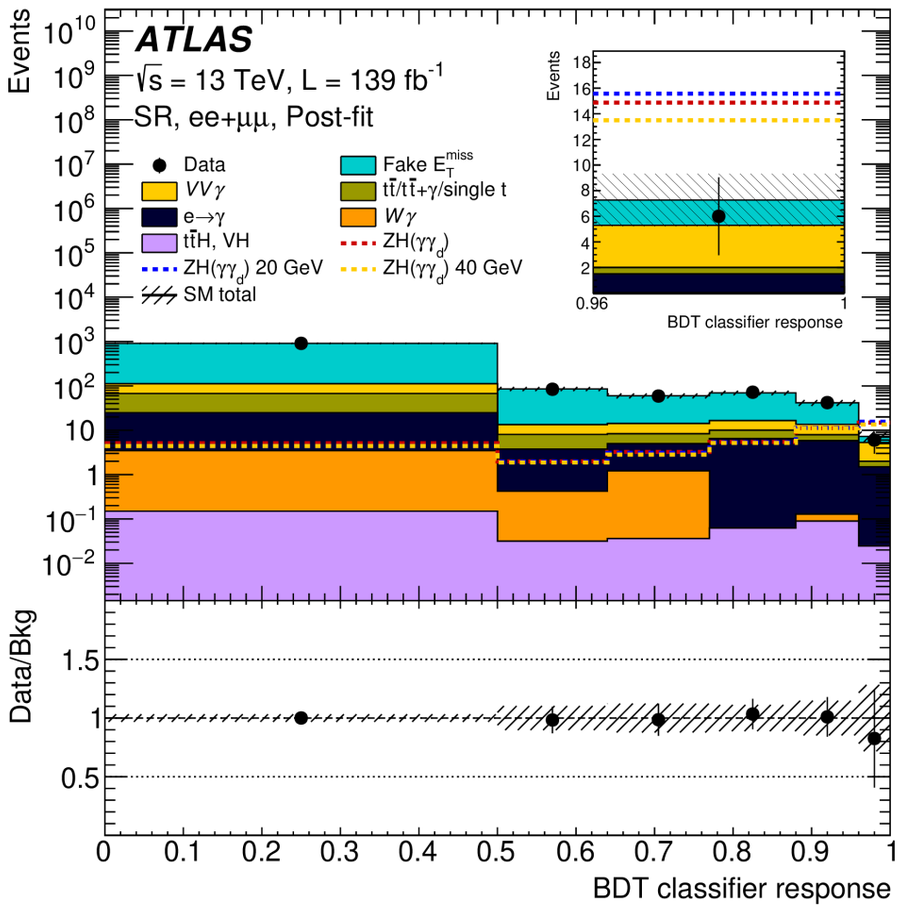

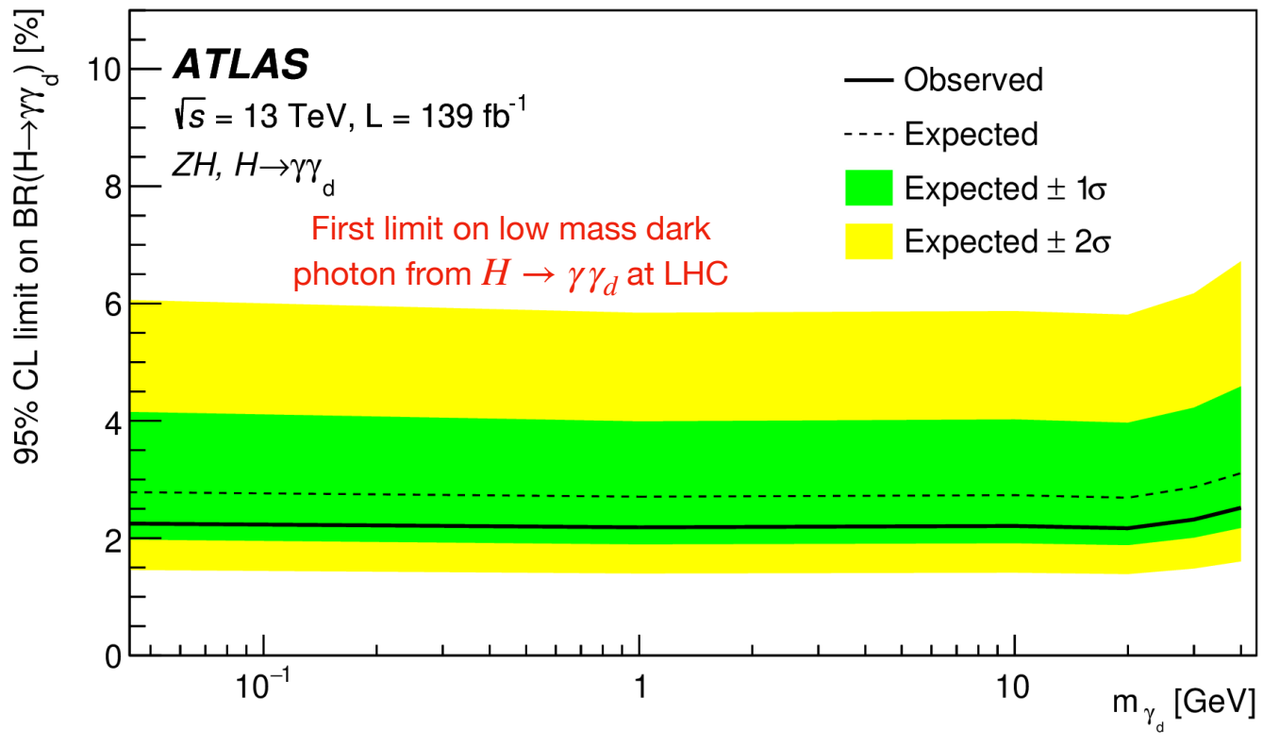

Production	ZH	VBF
ATLAS	2.3 (2.8)%	1.8 (1.7)%
CMS	4.6 (3.6)%	3.5 (2.8)%

Mono-photon re-interpretation for $H \to \gamma\gamma_d$

- reinterpretation of $E_{\mathrm{T}}^{\mathrm{miss}} + \gamma$ to search for dark photon in high-mass resonances.
  - $m_H \in [400,3000]$ GeV; massless dark photon;
  - dark photon $\to E_{\mathrm{T}}^{\mathrm{miss}}$.
- Include contribution from both VBF and ggF production modes.
- Discriminant variable: $E_{\mathrm{T}}^{\mathrm{miss}}$.

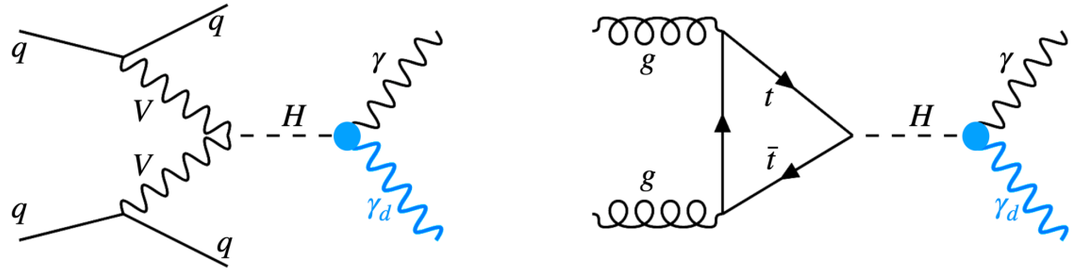

VBF ggF